Response of a threatened steelhead trout population to water-provisioning scenarios for the Carmel River, California

David A. Boughton, National Marine Fisheries Service, Southwest Fisheries Science Center, 110 McAllister Way, Santa Cruz, CA 95060, USA

Haley A. Ohms, University of California Santa Cruz, Santa Cruz, CA 95060, USA and National Marine Fisheries Service, Southwest Fisheries Science Center, 110 McAllister Way, Santa Cruz, CA 95060, USA

Summary

The links between stream flow patterns and adult steelhead production are unclear for the Carmel River. Here we fit generalized additive regression models to fish data from the river to understand the influence of flow on the survival and mean length of steelhead parr at the end of their first spring and summer, using about three decades of data. We also developed a spawner regression model to predict adult returns from the parr data, and then analyzed a variety of water-management scenarios relative to this baseline scenario. Scenarios included an unimpaired flow scenario, a dam-removal scenario, and two reservoir dredging scenarios. Among our key findings is that spring flow is the strongest driver of parr growth and median size at the end of summer, and parr growth in turn is a key driver of parr density via a self-thinning process. Both parr density and parr size at the end of summer were important predictors of adult spawner abundance two and three years later, when the parr would be expected to have reached spawning age. The main role played by summer flow appeared to be maintaining wetted area in the stream channel during the key bottleneck of the low-flow season, which gave greater space for the self-thinning process to play out. This maintenance of wetted area appeared especially consequential in the lower Carmel valley (west of the Narrows), which functioned mainly as habitat for larger steelhead parr, including age-1 parr. These larger parr then played an outsized role in the production of adult steelhead.

The unimpaired water scenario assumed the water table in the lower valley was high, resulting in greater wetted area and high numbers of large parr in this domain, which in turn generated large numbers of adult steelhead, especially in years with wet spring conditions. The unimpaired scenario also predicted lower flows in the rest of the mainstem during the summer, relative to the baseline. Dam removal scenarios assumed water conditions similar to unimpaired, except that the lower valley was routinely dewatered in the summer due to water withdrawals, similar to what has been occurring under the baseline scenario. Our analysis suggests that for a dam removal scenario, the gain in adult production from reconnecting the upper watershed was approximately equal and opposite to the loss of adult production due to lower summer flows without the dam. Reservoir-dredging scenarios produced modest gains in adult production, similar to the unimpaired scenario, but due mostly to maintenance of greater wetted area in the summer relative to the baseline. Maintenance of surface flow in the Lower Valley was at least as important as the effects of the dam on flows elsewhere. This assessment focused only on the immediate response of the population to surface flow, and did not examine the many other effects on habitat from the management of natural fluvial processes.

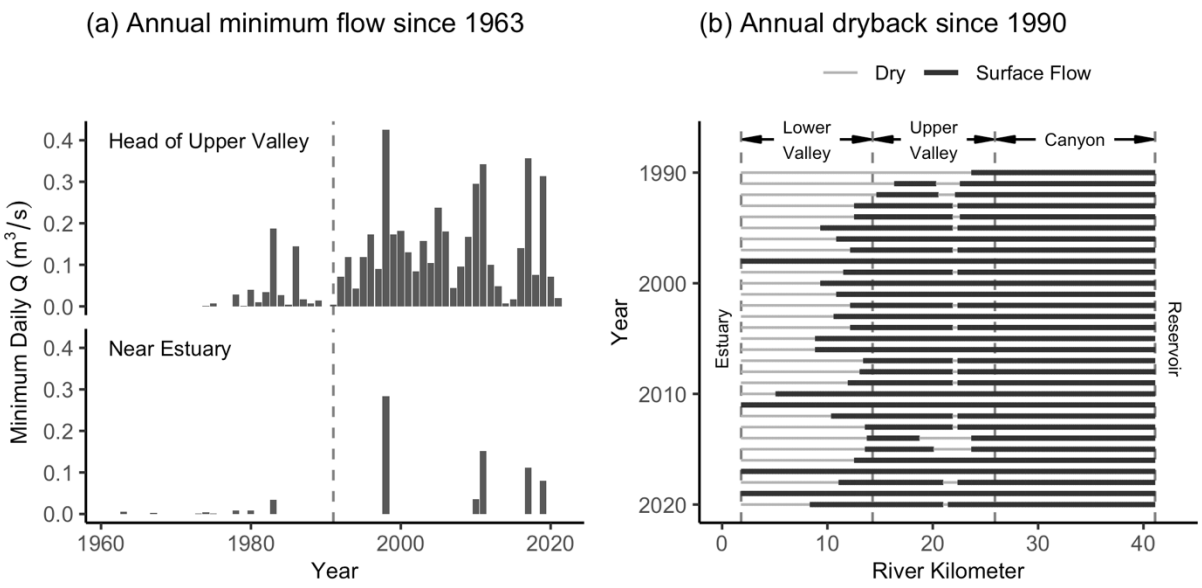

Figure 1. **(a)** Recent history of low-flow at the head and foot of Carmel Valley (Robles del Rio and Near Carmel gauges, respectively). **(b)** Spatial pattern of annual dryback in Carmel River downstream of Los Padres Reservoir, reconstructed for each year since 1990 from field notes from fish rescue operations.

Introduction

For much of the 20th Century, the water of the Carmel River and its aquifer was viewed mainly as a commodity resource to be stored in two reservoirs. During the dry season, streamflow downstream of the lower reservoir at San Clemente was simply seepage through the dam (Snider 1983), which infiltrated completely into the aquifer of Carmel Valley and left the alluvial portion of the river mostly dry most of the year. In the wet season, surface flow allowed migratory steelhead trout to ascend the river and a fish ladder at San Clemente Dam, spawning in upstream habitat where the river maintained perennial surface flow. But dewatering of the lower river, impediments to both upstream and downstream fish passage at the two dams, and various other factors substantially limited productivity of the Carmel steelhead population in this period.

Starting in the late 1970s, releases of reservoir water were modified to keep surface flow mostly above zero at the head of Carmel Valley (Figure 1a, top). But at the lower end of the valley near the estuary, it mostly continued to decline to zero due to infiltration into the lowered water table of the aquifer (Figure 1a, bottom). An exception was the extremely wet winter of 1981-82, which saturated the watershed enough to maintain a nontrivial surface flow in the lower river through the entire dry season. That year, Dettman and Kelley (1986) documented extensive rearing of juvenile steelhead throughout the river system, including large numbers in the usually dry channel of the lower river.

Ten years later, the river reached a turning point, when the management of its water was fundamentally changed to maintain more substantial surface flows at the head of the alluvial valley. Well operations were also changed to raise the water table and maintain surface flow upstream of the Narrows, a natural bedrock constriction that effectively separates the alluvial valley into two distinct groundwater basins. As a result, the annual dry-back of the river channel was confined mostly to the lower valley downstream of the Narrows (Figure 1b). Numerous other measures, such as restoration of riparian vegetation, fish rescues, captive rearing of wild

steelhead, gravel augmentation for spawning habitat, and eventually the complete removal of San Clemente Dam, were also pursued to promote steelhead recovery.

The Carmel River and its steelhead are now approaching a second turning point, with decisions pending on the fate of the remaining dam at Los Padres, as well as a future water-management strategy to balance the needs of people and the river's aquatic ecosystem. To provide scientific input on these decisions, we used data collected in the past 30 years to answer two related questions: First, how did steelhead production respond to the historical flow regime? Second, how strongly would alternative water-management scenarios for the river alter steelhead production if they had been implemented instead?

Because steelhead populations are affected by diverse environmental influences whose future unfolding is uncertain, we examine the water scenarios within the context of the recent past rather than the near future. This permits us to frame the response of the steelhead population to each water scenario in a quantitatively precise way, as a difference from its observed historical pattern of variation, which we call the "baseline scenario." Analyzing alternative scenarios relative to the baseline allows us to ask our second question using the answer from our first question, while holding all other environmental effects constant.

Methods

Study system

Carmel River drains a mountainous, 660 km^2 coastal watershed in California, where the nearby ocean generates a "Mediterranean" climate of warm wet winters and foggy, rainless summers. The surrounding coastal mountains generate a precipitation gradient, with high winter rainfall in the west and south (~1.7 m annually in some areas), and much more arid conditions in the north and east (~0.6 m annually). Adult steelhead, known as spawners, typically migrate up from the ocean to spawn January through April. Juvenile progeny, known as parr, typically remain in the river 1 year (sometimes 2 and occasionally 3), then transform into a saltwater-tolerant form known as smolts and migrate down to the ocean in April or May (Arriaza et al. 2017). After 1 or 2 years in the ocean (rarely 3 or 4) they return to the river to spawn. The freshwater-resident form of *O. mykiss* (rainbow trout) also occurs in this system and interbreeds with steelhead. The abundance of rainbow trout has not been formally measured, but observations suggest a relatively modest yet consistent presence.

Data for addressing our questions cover ~30 years, and come from a series of stream gauges (Figure 2) and annual population surveys of the steelhead (Arriaza et al. 2017). Population surveys include spawner counts from fish-passage infrastructure at two dams, and parr data collected at the end of the dry season in September and October. Parr data comprise fish densities (m^{-2}), fork lengths (of sampled fish), and channel wetted widths, from depletion-sampling at a series of sample reaches described in more detail below.

Although we focused on effects of stream flow, we must statistically control for effects of two related fish-conservation activities. To mitigate the impacts of lost surface flow, parr are routinely rescued from drying stream reaches each summer by the Monterey Peninsula Water Management District and the Carmel River Steelhead Association. These fish have two distinct fates. Some are taken to a steelhead rearing facility, held and fed until the wet season, and then released as downstream migrants. Others are immediately relocated to another part of the stream network that has maintained surface flow, and released. We call these groups captively-reared and rescued fish, respectively, and incorporate them into the analysis as appropriate. But they are not our focus here.

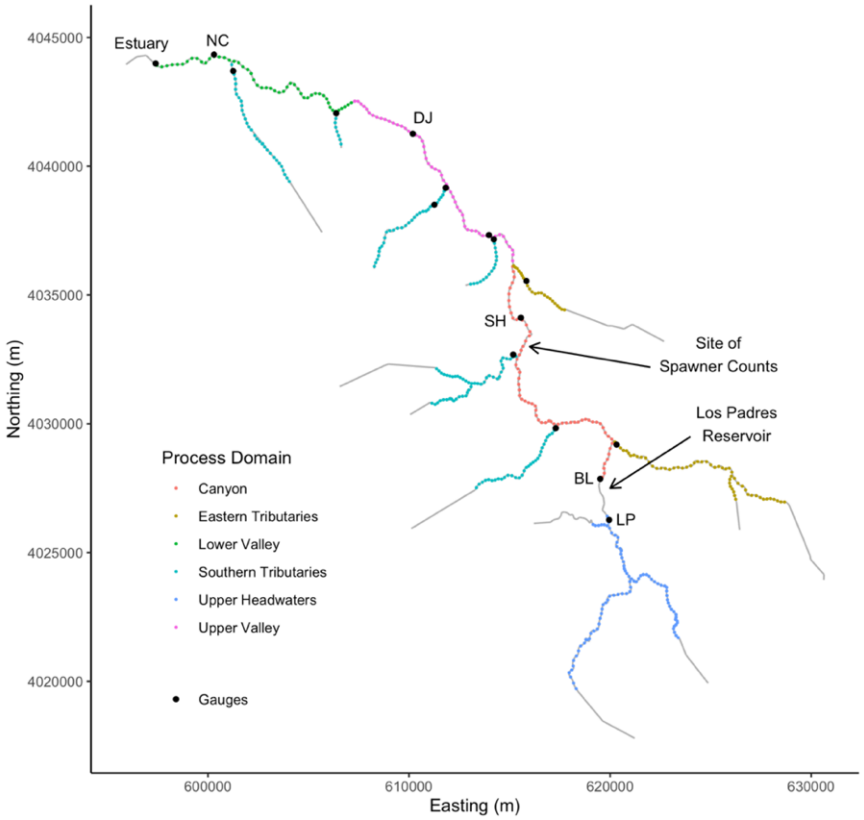

Figure 2. Carmel River and tributaries, with locations of stream gauges (black dots), midpoints of sample reaches in the finite sampling frame (colored dots), and associated process domains (colors). Stream segments without dots are either above impassable barriers or are lentic habitats (estuary, reservoir). Two-letter codes refer to mainstem stream gauges mentioned in the text.

Analytic strategy

Our general strategy was to use a statistical parr model to predict how stream flow affected wetted area, parr density, and parr size at the end of the dry season; and then to use a statistical spawner model to predict adult abundance from the wetted area, density, and size. Once these models had been calibrated to the historical baseline, we constructed a variety of alternative flow scenarios and predicted their effect on adult production, relative to baseline and holding all other aspects of population dynamics constant. The latter aspects included the compounding effects of population growth across years, and so the predicted responses represent a "one-at-a-time" test, where the response in each year represents a scenario of altered flow in that year, but baseline flow patterns otherwise. Each year thus represents a statistically-controlled independent trial.

Our statistical approach used generalized additive models (GAMs) for their flexibility in characterizing the empirical relationships between predictors and responses (Wood 2017). The approach championed by Wood (2003, 2004; Wood et al. 2016; 2017) uses thin-plate regression splines penalized by smoothing parameters to flexibly estimate response curves (partial effects) that optimize out-of-sample prediction. Since our goal was prediction rather than inference, we also used AIC to sort among models with competing predictors (Tredennick et al. 2021). AIC (Akaike Information Criterion; Burnham and Anderson 2002) is designed to identify models that optimize out-of-sample prediction, and so is appropriate to predicting novel scenarios.

All such analyses used the computer software package R (R Development Core Team 2021) and the add-on package mgcv (Wood 2017), in which we computed AIC from the maximum likelihood and the effective degrees of freedom (*edf*) returned by the function mgcv::logLik.gam. In general, we discuss AIC in terms of the evidence ratio (ER; Burnham and Anderson 2002), which derives from the difference of AIC between two models (Δ_{AIC}) but is more intuitive in our view. We interpret the ER of two models as the odds that one versus the other makes better out-of-sample predictions.

For simplicity, we assumed the effects of flow to be predictable from an annual summary statistic. We considered eight statistics total: For each of two seasons, spring (Mar-May) and summer (Jul-Sep), we considered two alternative measures of central tendency (mean and median) and two measures of seasonal extremes (10^{th} percentile and 90^{th} percentile of daily flow). Central tendencies describe the overall stream conditions for each season, while extremes describe the stresses imposed by high or low flow. Because the eight metrics were correlated, we considered them to be mutually exclusive candidates for prediction and selected the best one using AIC. This avoids the well-known hazards of interpreting multiple regression on correlated predictors (McElreath 2020).

To capture habitat heterogeneity, we modeled effects of flow on fish within the context of process domains (Figure 2). Process domains are spatially identifiable areas characterized by distinct suites of fluvial processes (Montgomery 1999), and the numerous stream gauges allowed us to compute flow metrics local to each such domain. Following Montgomery (Montgomery and Buffington 1997; 1999), we divided the stream network into a headwater/tributary section; a middle canyon section; and an alluvial valley section, corresponding to reaches where channel morphology is dominated by sediment export, transport, and deposition, respectively. In addition, for the tributaries we distinguished between those that receive high rainfall (Upper Headwaters, Southern Tributaries in Figure 2) versus low rainfall (Eastern Tributaries).

Finally, we further distinguished process domains based on spatially distinct but pervasive human impacts. We separated the otherwise similar Southern Tributaries from the Upper Headwaters, because the latter is above Los Padres Reservoir, which blocks passage of 80% or more of outmigrating steelhead annually (Ohms et al. 2022), and also likely impacts upstream passage of adults during the trap-and-haul procedure. We also separated the Upper and Lower Valley (alluvial river channel upstream and downstream of the Narrows, respectively). The local water company has well fields for extracting groundwater throughout both the Upper and Lower Valley, but since 1992 it has pumped water each summer from the aquifer near the estuary at the west end of Lower Valley, with well operations gradually moving eastward each summer as necessary to maintain water supply. This practice generally maintained a high water table and mostly perennial surface flow in the Upper Valley, but a pattern of seasonal drying in the Lower Valley (Figure 1b). A small section of braided channel in the Upper Valley also tends to dry most summers (visible in Figure 1b), due to deposition of sediment at a local knickpoint in the channel gradient.

The Parr Model

Parr data came from a set of index reaches and randomly-sampled reaches. Since 1991, the local water district sampled ~10 index sites annually, broadly distributed across Canyon, Upper Valley and Lower Valley, while the state sampled three index sites in Upper Headwaters about every five years. In 2015 we established a finite sampling frame across all process domains (Figure 2), and randomly sampled 10-20 additional reaches yearly using a rolling panel design (Adams et al. 2011; Boughton et al. 2022). In all cases, parr density (fish/m^2) was estimated for

stream sections ~100m long using block nets, electrofishers, and the depletion method (Temple and Pearsons 2007; Reynolds and Kolz 2013), with abundance estimated as in Carle and Strub (1978; Ogle et al. 2021a; Ogle et al. 2021b). We found no significant differences in parr density between index and random reaches (Boughton et al. 2020) and here treat them as exchangeable.

For realism, we modeled parr as a multivariate response consisting of parr density, parr size, and the wetted width of the sample reach, with density log-transformed to stabilize variance. Parr density and size showed a clear negative correlation across sampling events (Figure 3), which is an expected result of competitive self-thinning processes in freshwater salmonids (Dunham and Vinyard 1997; Einum et al. 2006; Rosenfeld 2014; Myrvold and Kennedy 2015; Matte et al. 2020). Self-thinning typically involves fish movement as well as mortality and can thus redistribute fish across the watershed, away from areas with large fish defending large territories (Grant and Kramer 1990). Fish density and size are thus mechanistically linked, along with wetted area which sets the total space for the competitive processes to play out (Grant et al. 1998; Ayllon et al. 2012).

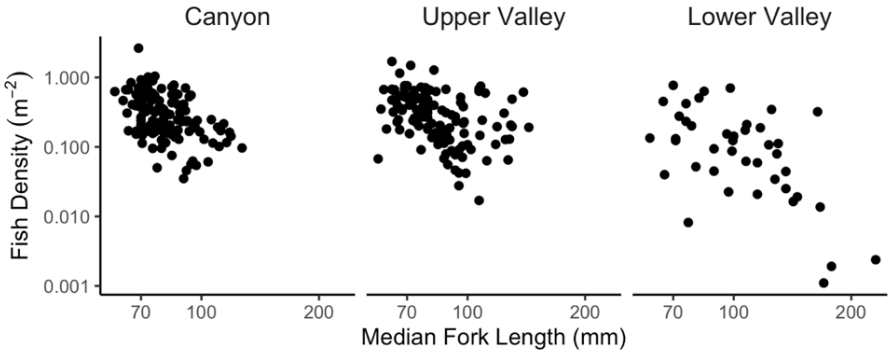

Figure 3. Density and median size of parr, for sampling events on the mainstem downstream of Los Padres Reservoir.

Streamflow should affect self-thinning, but the most predictive flow metric is unclear since thinning arises from a variety of ecological mechanisms (Matte et al. 2020), and can also be amplified by asymmetric competition (Hughes 1998). The number of spawners should also affect parr production, and thus their density and size, and so should the number of rescued fish each summer, as well as myriad other impacts that would vary unpredictably among years and stream reaches. We treat the latter as random effects, so that the full parr model has the structure

$$\text{Eq. 1} \quad \ln(\text{Density}) = \begin{matrix}\text{Mean for}\\ \text{process}\\ \text{domain}\end{matrix} + \begin{matrix}\text{random}\\ \text{effect of}\\ \text{year}\end{matrix} + \begin{matrix}\text{random}\\ \text{effect of}\\ \text{reach}\end{matrix} + s(\text{flow}) + s(\text{spawners}) + s(\text{rescues})$$

$$\text{Eq. 2} \quad \text{Fish Length} = \begin{matrix}\text{Mean for}\\ \text{process}\\ \text{domain}\end{matrix} + \begin{matrix}\text{random}\\ \text{effect of}\\ \text{year}\end{matrix} + \begin{matrix}\text{random}\\ \text{effect of}\\ \text{reach}\end{matrix} + s(\text{flow}) + s(\text{spawners}) + s(\text{rescues})$$

$$\text{Eq. 3} \quad \begin{matrix}\text{Wetted}\\ \text{Width}\end{matrix} = \begin{matrix}\text{Mean for}\\ \text{process}\\ \text{domain}\end{matrix} + s(\text{year}) + \begin{matrix}\text{random}\\ \text{effect of}\\ \text{reach}\end{matrix} + s(\text{flow})$$

where "s(x)" represents a spline curve for predictor x, and random effects are normally distributed with mean zero (function mgcv::s with bs="re"; see Wood 2017 §3.5.2).

Exploratory analysis suggested two refinements. First, the effect of year on wetted width was modeled as a smooth curve rather than a random effect, to represent geomorphological change across years. Second, the effect of rescues (number of rescued fish released into a given domain in a given year) was modeled as the sum of a categorical effect and a spline curve. The categorical parameter was fit to an indicator (True/False) for whether a given domain received fish in a given year, while the spline curve modeled the quantitative response of density to the number of released fish, which varied greatly.

We added the categorical effect because we observed that density in a domain was systematically lower in years when they received rescues versus not; yet density also had an opposite, positive association with the (nonzero) number of released fish. We interpret these opposing patterns as stemming from inhibited parr movement in dry years—that the same conditions generating stranded fish also prevented fish from moving out of drying reaches into reaches with perennial flow but low occupancy. The categorical effect thus represents the negative impact of inhibited movement, while the spline curve represents the ability of rescues to mitigate it.

We represented parr length as the median fork length of fish caught in each sampling event. Histograms of these lengths typically had a dominant mode, interpreted as the most common age class in the sample, and often one or occasionally two smaller modes representing other age classes. We used median size rather than mean to better represent this dominant mode, so that Eq. 2 modeled the most common age class in each sample site. Ergo, any distinct dynamics of other age classes were implicitly absorbed into the random effects, and thus held constant among the various scenarios. The dominant mode usually represented age 0 fish, but occasionally age 1 fish or even adult rainbow trout (*cf* Figure 3).

Finally, to predict the length of wetted channel in the Upper and Lower Valley, we used the dry map (Figure 1b) to fit a one-parameter model,

Eq. 4
$$p_w = 1 - e^{-kQ}$$

in which p_w is the proportion of total channel length that maintained surface flow all summer, Q is the flow metric, and k is a single fitted parameter. Here, zero flow at the gauge corresponded to zero proportion of wetted channel, the steepness of response to Q is described by k, and the equation asymptotes at 1 for large Q.

Eq. 1 through Eq. 3 define a generalised additive mixed-effects model, where observations are individual reaches, but predictors are grouped by process domain and year, treated as fixed and random effects respectively. A mixed-effects model is well suited to our dataset with its unbalanced samples across years, because years with fewer data will automatically get "shrunk" toward the overall mean of each domain, rather than bias our estimates of the means and the splines (Gelman and Hill 2007). Our data is also unbalanced across domains, which we dealt with by selecting model structure using only the domains sampled every year—Canyon, Upper Valley and Lower Valley—which are also the ones that can vary among the scenarios. Once the final structure had been selected via AIC, we added back observations for Upper Headwaters and Southern Tributaries and refit the model. We omitted the arid Eastern Tributaries because nearly all randomly-sampled reaches had zero surface flow. The role of the lagoon is not modeled explicitly due to lack of data, and thus is subsumed into the annual random effects.

The parr model's final structure was selected in three steps. First, we constructed univariate versions of Eq. 1 through Eq. 3 with each of the eight flow metrics, and used AIC to select the most predictive metric for each. Then, we removed any predictor if it improved AIC. Finally, we

created the multivariate normal model and used AIC to compare the four possible combinations of flow metrics previously selected for Eq. 1 and Eq. 2. We assume this identifies the best out-of-sample predictors after accounting for correlation of fish density and size.

The Spawner Model

Spawner counts came from a fish ladder at San Clemente Dam. These counts omit fish spawning downstream of the dam, but in our view are reliable indicators for relative abundance and average 57% of total run size (see Supplement §S1, §S2). The dam was removed in 2015 and newer counts were inferred from correlated counts at Los Padres Dam (Supplement §S3).

The spawner model predicts adult returns from parr abundance and size at the end of the dry seasons two and three years prior. According to fish scales (Dettman and Kelley 1986), most returning adults spend one or two years in the ocean, or in other words, are survivors of this parr group from two and three years prior. The model used simple linear regression with the intercept fixed at zero, because we know that zero parr produce zero adults, and the slope of the regression is then interpretable as ocean survival.[1] To maintain this interpretation when size was a second predictor, it was centered on zero (mean subtracted). Parr abundance and size for each year came from the parr model, predicted for all reaches in the sample frame and then aggregated (sum for abundance, abundance-weighted mean for size). For accuracy we included captively-reared parr in this calculation, and also removed 80% of the parr estimated for Upper Headwaters because a tagging study estimated that 80% of downstream migrants disappear into Los Padres reservoir, possibly due to predation (Ohms et al. 2022).

Parr abundance is an obvious predictor of spawner abundance, but the role of size is less clear. Usually, larger smolts tend to survive better in the ocean and thus increase spawner abundance (Ward et al. 1989; Bond et al. 2008), but this advantage can be erased by poor ocean conditions (Ward 2000), and in any case propensity to smolt is a complex function of parr size that declines for parr > 150 mm and also depends on sex, genotype, age class and other factors (Satterthwaite et al. 2009; Pearse et al. 2019). Our size predictor averages across all this heterogeneity so its predictive value is unclear. We considered three model structures for its role (Figure 4). In our view, model J × L is the most biologically realistic, but also has the most parameters and therefore the highest risk of overfitting.

We also considered models that split vs lumped the two years of parr. Splitting allows survival to depend on years spent in the ocean, while lumping benefits from fewer parameters.

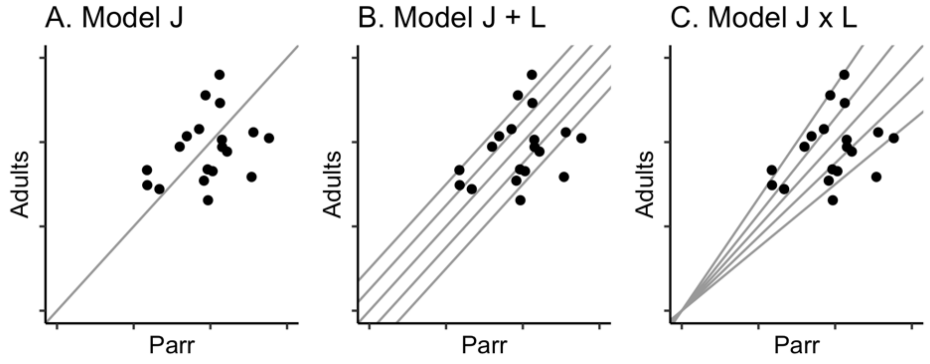

Figure 4. Schematic of prediction structures considered for the spawner model, where multiple lines indicate groups of parr with different mean-median lengths.

[1] More accurately, apparent survival since it omits fish spawning downstream of San Clemente Dam.

Flow scenarios

Carmel River is an extremely well-gauged system, with daily streamflow gauges on all major tributaries and six gauges on the regulated mainstem (Figure 2). A seventh mainstem site immediately upstream of Los Padres Reservoir represents natural flow (LP in Figure 2). Unfortunately flow at this site was only measured monthly and not during the height of each wet season, except in 1995 and 1998. In these two exceptionally rainy years, flow was estimated daily during the wet season.

We used the gauge data to construct six flow scenarios (Table 1). The "baseline scenario" represents the actual historical situation of the past 30 years, while the other scenarios span a range of possibilities for the local water company to exercise its water right, from complete absence of any water extraction (the unimpaired scenario) to expansion of the existing water right by dredging more capacity in Los Padres Reservoir. In the baseline scenario, the water company routinely exceeded its legal water right of 3376 acre-feet per year to meet demands of people; scenario CDO/3376 assumes the limits of the water right were respected but otherwise matches the baseline. In all scenarios except unimpaired, the water right was exercised at well fields in the Lower Valley. Of course, numerous other water users in the watershed have their own wells and their impacts are implicitly held constant across scenarios.

Table 1. Flow scenarios and methods for constructing them

Scenarios	**Description**[1]
Baseline	Historical pattern, water right 3376 routinely exceeded.
Unimpaired	No dams, no water extraction by water company.
LP Dam Removal	No dams, water right 3376 exercised.
CDO/3376	Historical pattern, except water right 3376 not exceeded.
LP Dredge/3906	Water right expanded by reservoir dredging.
LP Dredge/4492	Water right expanded by reservoir dredging.
Methods	
BHM Methods	Output from Basin Hydrologic Model
Daily BC	Bias-correction applied to daily flow data.
Seasonal BC	Bias-correction applied to seasonal flow metrics.
Empirical Methods	Regression models predict downstream gages from upstream gages.
High infiltration	Lower Valley infiltration predicted from Lower Valley regression
Low infiltration	Lower Valley infiltration predicted from Upper Valley regression

[1] Numbers 3376 etc. are annual acre-feet of water extraction covered by the water right of the local water company.

Scenarios were constructed using a variety of methods, summarized in Table 1. BHM methods used outputs from a process-based "basin hydrologic model" that covered hydrologic processes for the entire Carmel watershed, including runoff, stream flow, groundwater, and evapotranspiration. Outputs were provided by the Monterey Peninsula Water Management District and their methods and assumptions are not reported here. Empirical methods used regression to predict flow at downstream gauges from flow at upstream gauges, except for the empirical baseline, which simply used the gauge data itself.

The empirical and BHM versions of the baseline scenario would ideally be the same, but in fact were quite different—especially in the Lower Valley where the BHM scenario greatly underestimated infiltration and channel drying in late summer. These differences mean the BHM outputs were biased, which we corrected using:

$$\text{Eq. 5} \quad \text{Bias-Corrected Scenario X} = \text{Modeled Scenario X} - \text{Modeled Baseline Scenario} + \text{Empirical Baseline Scenario}$$

Eq. 5 assumed that all bias in model outputs was captured by the difference between the two versions of the baseline scenario. The bias-corrected baseline is thus identical across methods, and each other scenario can be represented simply as a deviation from it. We compared two versions of bias-correction (BC). The daily BC applied Eq. 5 to daily flow before aggregation into the seasonal metrics used by the parr model, while the seasonal BC applied it after aggregation. An additional statistical correction was needed to account for infiltration in Lower Valley, due to an abundance of zeros in the empirical baseline. The correction assumed a fixed infiltration rate during the dry season, estimated from the difference between Upper Valley and Lower Valley flows (see Supplement §S4 for details).

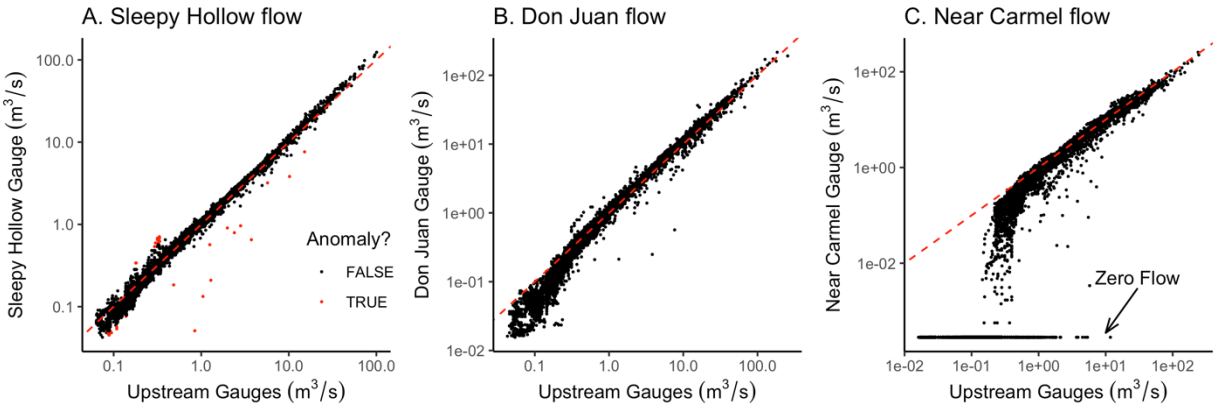

Figure 5. Upstream gauges as predictors of daily flow at stream gauges representing the Canyon domain (**A**), the Upper Valley domain (**B**), and the Lower Valley domain (**C**). Red dashed line references an idealized 1:1 relationship. Anomalies at the Sleepy Hollow gauge (marked as red in **A**) were assumed to be due to filling or discharge of San Clemente Reservoir, and were removed before fitting regressions. Downward curvature of the point cloud at low flows in (**B**) and especially (**C**) are assumed to be effects of infiltration into the aquifer under Carmel Valley.

For empirical scenarios, we constructed at-a-station GAMs to predict downstream gauges from summed flow at upstream gauges (Figure 5). These methods used AIC to consider additional predictors for loss or gain of surface flow: mean or maximum daily air temperature, day-of-year (DoY), year, and various two-way interactions. Air temperature[2] can drive substantial evaporative losses from the stream, especially in the dry season. Day-of-year captures seasonal effects of unmeasured drivers such as soil moisture; and year captures the component of such drivers that spans multiple years, such as the deep depletion of soil moisture in an extended drought. This parsing of unmeasured environmental factors as implicit year and seasonal effects follows O'Donnell et al. (2014).

All at-a-station models had log-transformed flow to stabilize variance, and all except Lower Valley assumed a Gaussian location-scale model, which is like a normal model but also has a linear predictor for residual variance. We made upstream flow a predictor of the variance to

[2] From PRISM Climate Group, Oregon State University, https://prism.oregonstate.edu, dataset AN81d, accessed 20 Jan 2022.

capture the higher variance at lower flows that is visible in Figure 5. Lower Valley required a left-censored normal model (R package cenGAM::tobit1) to accommodate the numerous days of zero flow (Figure 5C). The censoring point was set at the smallest non-zero flow detectable by the gauge (0.00028 m^3/s). The LP gauge above Los Padres Reservoir was crucial for scenarios of natural flow (unimpaired, dam-removal), but had only monthly data and no upstream gauges, so we filled in the gaps using a GAM with gauge data from a nearby river as a predictor. Of three candidates (nearby Carmel tributaries; Arroyo Seco River to the south east; Big Sur River to the south west), AIC indicated Big Sur River flow was by far the best predictor.

The empirical versions of the unimpaired and dam-removal scenarios simply replaced the flow pattern below Los Padres Reservoir with the pattern directly above it (gauges BL and LP in Figure 2). We then used at-a-station models to propagate the effects downstream to the Canyon, Upper Valley and Lower Valley (gauges SH, DJ and NC in Figure 2), adding in tributaries along the way. Likewise, the various dam-fix scenarios took BHM output for the Canyon, bias-corrected its daily flows, and then propagated them downstream using the at-a-station regressions.

The empirical method has no straightforward way to represent infiltration in the Lower Valley under various water-extraction scenarios, and so we bracketed the range of likely response with a high-infiltration method and a low-infiltration method (Table 1). The former is same as baseline, where the legal water right was routinely exceeded by large margins, while the latter predicted flow at Lower Valley using upstream gauges plugged into the regression model for Upper Valley. In practice this meant that the curvature observable in the point cloud at lower left in Figure 5B replaced the sharper curvature observable in Figure 5C.

Population response to flow scenarios

The streamflow metrics for the various scenarios were plugged into the parr model to predict total parr abundance and mean-median fork length for each year that had BHM outputs (1993 to 2015). We then used parr abundance and length in the spawner model to predict adult returns per brood year of parr. To control for the effects of all the various other background influences on population dynamics, we summarized each scenario as its effect relative to the baseline scenario.

Uncertainty was propagated during this procedure via multiple imputation. We treated the estimated parameters from the parr model as posterior Bayesian probability distributions (see Wood 2017 §6.10 and §7.2.7). Uncertainty was propagated via 5000 simulated draws from the posterior, with each draw held constant across scenarios. Likewise, random effects and residual error for unsampled reaches were simulated 5000 times and held constant across scenarios. For each of these posterior draws, total parr abundance and size was calculated for each year of each scenario. Then, a new estimate of the spawner model was imputed using the parr abundance and size from the baseline scenario. This produced draws from an approximate posterior for the spawner model, which were then used to predict spawner abundance under the other scenarios.

Results

Parr model

Spring low-flow (QP_{10}) was the best predictor for parr length (*i.e.* had the lowest AIC value), and summer median flow (QP_{50}) was the best predictor for parr density. The evidence ratio was 10:1 over the next-best model, which had summer median flow for both fish length and density. In the best parr model, correlation of the error terms for parr size and density was -0.40, substantial enough to establish an important role for self-thinning.

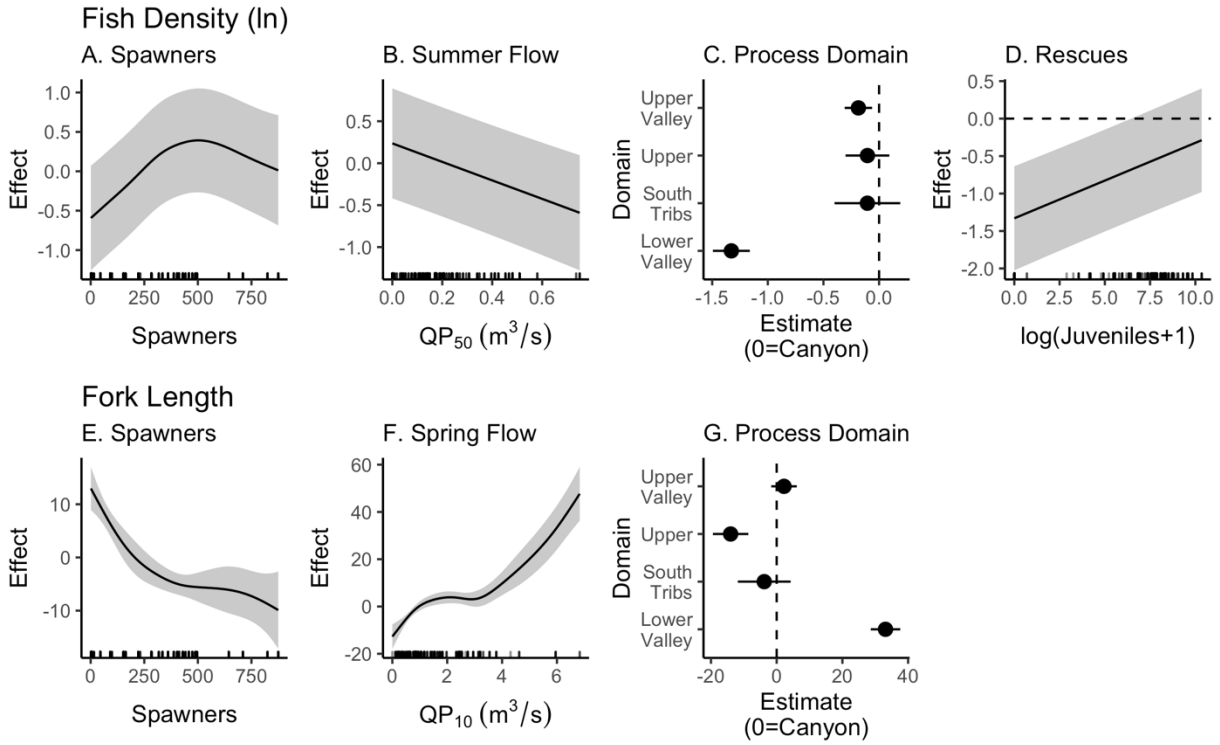

Figure 6. Partial effects of predictors for fish density (top) and size (bottom) in the parr model. Effects for fork length are directly interpretable as millimeters of size achieved (or lost), relative to the mean size in the Canyon domain (84 mm). Effects for density are on the scale of natural logarithms (1 unit ≈ three-fold change), relative to mean density in the Canyon (~ 0.5 fish/m^2). Shading is 67% confidence bands, and hashes on the x-axis plot the predictor data.

Figure 6 shows partial effects estimated by the parr model. In the first column, the effect of spawners on parr density (Figure 6A) showed a classic hump-shaped stock-recruit curve, peaking around 500 spawners. A likely competitive effect also showed up for parr length (Figure 6E), where the fork length achieved by parr drops sharply by ~15 mm as spawner abundance rises from single digits to ~300 adults; its drop then moderates somewhat but still loses another 5 mm.

The effect of spring flow on growth is quite striking (Figure 6F). Initially, as spring low-flow (QP_{10}) rises from nearly zero to 1.5 m^3/s, parr size improves by about ~12 mm but then levels off. But the occasional years substantially wetter than 3 m^3/s produced huge effects, up to 50 mm of additional growth. For density, greater summer flow was associated with lower density, about a 2-fold decrease (Figure 6B). This seems counterintuitive if higher flow were associated with better survival, but is consistent with two alternative explanations, a strengthening self-thinning process and/or a dilution effect. For self-thinning, the combined patterns in panels B and F

suggest that wetter years produce faster growth, and the larger fish establish larger feeding territories (Grant and Kramer 1990), driving a lower density as smaller fish either emigrate or die (Hughes 1998). In the wettest years, the estuary stays connected to the mainstem, opening a food-abundant destination for emigrants in the summer when food is otherwise very limited (Bond et al. 2008; Kelson and Carlson 2019). However, experiments with adding a categorical variable for estuary connection in a given year (Yes/No) neither improved the model AIC, nor produced a stastically significant effect, so a specific role of estuary connection was not discernable in the data.

Panels C and G show mean density and size in the various process domains, relative to their means in the Canyon (0.54 fish/m^2 and 83.8 mm FL). The only statistically significant differences from the Canyon were size in the Upper Headwaters ($p = 0.0095$), and both size and density in the Lower Valley ($p < 0.0001$ for each). Parr were about 14 mm smaller in the Upper Headwaters than in the Canyon, and about 10 mm smaller than in the Southern Tributaries, which have comparable rainfall and geomorphic processes. Fish in the Lower Valley were considerably larger and less dense than anywhere else, on average 31 mm larger and 1/3 as dense as in the Upper Valley just upstream.

Finally, Figure 6D shows the effect of rescued fish on density, where the sloped line implies that number of released fish was log-linearly associated with higher densities at end of summer. The intercept of this line shows the magnitude of the categorical parameter, interpreted as density if fish were stranding but not rescued. Both the categorical and spline predictors were highly significant ($p < 0.0002$), showing that fish relocations partially reversed the impacts of stranding.

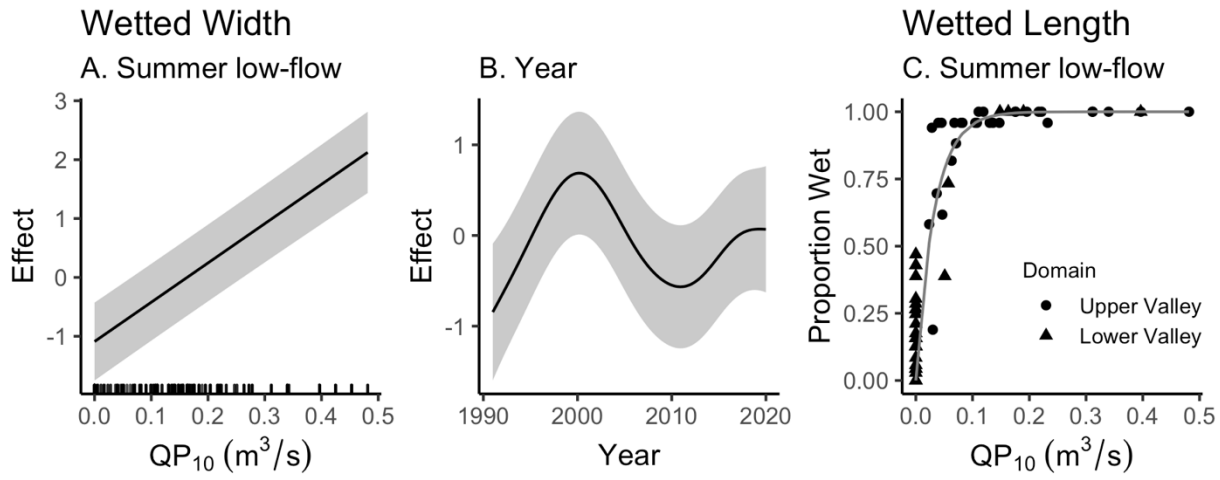

Figure 7. Partial effects for predictors of wetted width (**A, B**) and length (**C**) of stream habitat at the end of the dry season. In **A** and **B**, partial effects are directly interpretable as meters of width relative to the average in the Canyon (7.3 m).

Unsurprisingly, the best predictor for both the wetted width (Eq. 3) and wetted channel length (Eq. 4) was summer low-flow (QP_{10}). Response curves (Figure 7) showed striking patterns. Overall, wetted width responded linearly to summer low-flow, expanding by ~2 m as summer low-flow expanded from ~0.01 to 0.3 m^3/s (Figure 7A), or about ±15% of the mean width in the Canyon (7.3 m). The only process domain with a statistically significant difference in width was the South Tributaries ($p = 0.0043$). Unexpectedly, wetted width showed a complex

trajectory over the course of the 30 years (Figure 7B). Since effects of wet years versus dry years would be captured by QP_{10} in the first panel, this trajectory would seem to reflect true geomorphic change in the river system.

Proportion of wetted channel length (Figure 7C) was modeled more simply, as a one-parameter nonlinear model. The channel stayed mostly connected when $QP_{10} > 0.15$ m^3/s.

Spawner model

According to AIC, the top-ranked spawner model had both the most biologically plausible structure (J × L) and the most parsimonious lumping scheme for biennial parr groups (Table 2). Relative to models with distinct survival for fish staying one vs two years in the ocean, this top-ranked model was at least 800 times more likely to make better predictions, and 300 times more likely than a model ignoring parr size. Size matters, but not the residence time in the ocean apparently.

Table 2. Selection of the spawner model.

Model Structure	**Parr Groups**	**K**	**Δ_{AIC}**	**ER**
J × L	Lumped	4	0	1
J + L	Lumped	3	2.24	3.1
J	Lumped	2	11.4	300
J	Split	3	13.4	800
J + L	Split	5	18.1	8600
J × L	Split	7	22.9	92000

In the best spawner model (see Table S3), the coefficient for the J predictor (parr abundance) was 0.00181±0.00014, interpreted as the adult return rate per year for a parr group of average fork length (81 mm). However, the model assumed each parr group generates two years of adult returns, and the spawner counts at San Clemente are biased low (0.57 of total, see §S2), so after adjusting for these effects the best estimate for marine survival is 0.00635±0.00035; or in other words, 157 end-of-summer parr (1 ÷ 0.00635) produce one adult steelhead, on average over the entire baseline period. Note that this definition of marine survival also includes pre-emigration winter mortality and smolting rate.

Marine survival is quite sensitive to the average size of the parr group (Figure 8A). For the group with the smallest parr (67 mm), marine survival would drop from 0.64% to 0.14%, but for the year with the largest parr (95 mm), it would rise to 1.12%, an 8-fold range in expected marine survival.

Figure 8B shows combinations of abundance and fork length that give similar expectations for adult returns (isoclines), along with the actual returns that were used to fit the model (spawners). Over the past 30 years the population has wandered widely through this prediction space, showing that medium runs (200-400 spawners) were generated both by years with many small parr and years with fewer large parr. But to get the truly largest runs you need those wet years that generate large numbers of large parr.

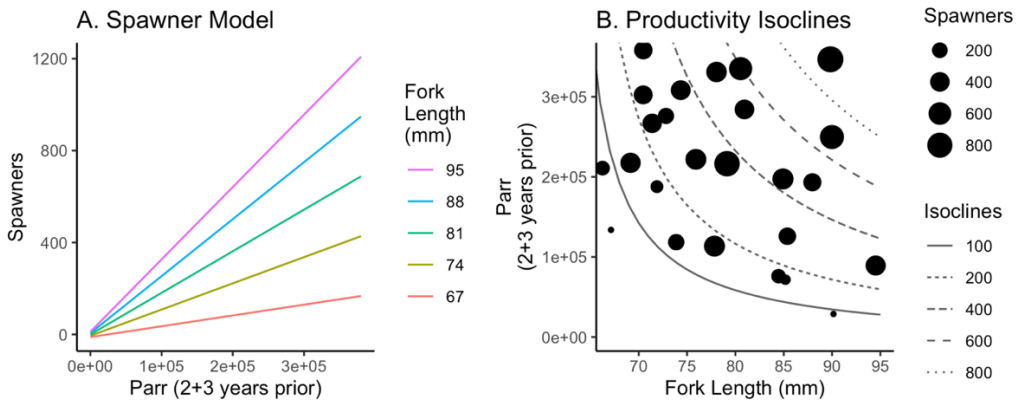

Figure 8. Two visualizations of the spawner model. (**A**) Predicted spawners at San Clemente per year for various fork lengths of parr two and three years earlier. The slope of each line represents annual return rate of spawners. (**B**) The same predictions shown as isoclines in the predictor space, with training data (dots) superimposed.

Empirical water scenarios

Details of the at-a-station regression models are not reported here, but complete graphs of partial effects and reconstructed hydrographs are in the supplement (§S5). These regressions were fit with huge datasets (~10,000 observations per gauge) and typically explained >99% of variation on the log scale.

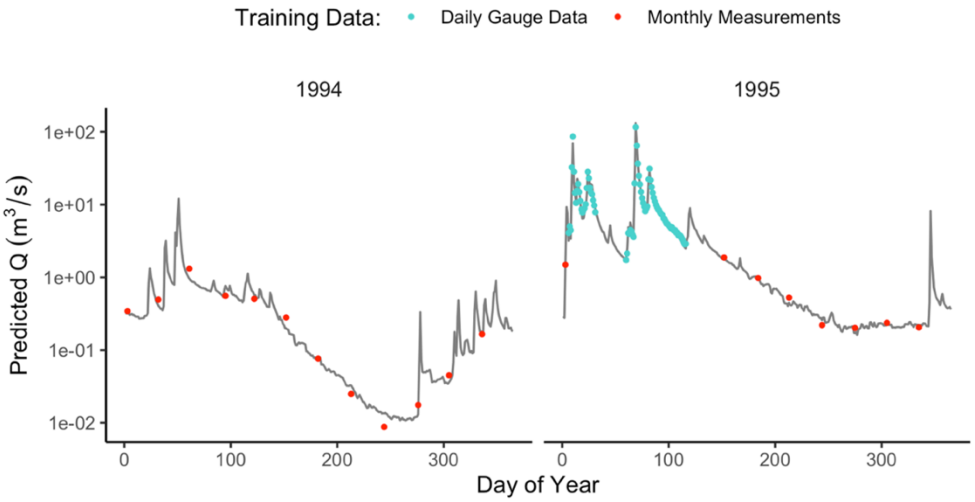

Figure 9. Unimpaired flow, as inferred for selected years at Los Padres Reservoir. Shown are a very dry year (1994) and a very wet year (1995). Predicted flow (gray) is from a regression of measurements upstream of the reservoir (red, blue symbols) onto the daily flow of the Big Sur River to the south west, as well as air temperature, annual, and seasonal effects.

The at-a-station model for natural flow above Los Padres is especially important, because it drives the scenarios for dam-removal and unimpaired flow, yet only had monthly data for most years. Figure 9 shows reconstructed hydrographs for a very dry and very wet year (See Figure S7 for the full reconstruction). The regression generally did a good job of predicting late spring and dry season flows (red dots vs gray line in Figure 9). It did over- or under-estimate the lowest flows in some years (see Figure S7). Figure 9 on the right shows one of two years when daily observations were made in the wet season (blue dots); these and monthly observations (red dots)

were highly correlated with daily flows in Big Sur River, which were therefore used to infer the detailed patterns observed in the gray line.

The dam-removal flow pattern had three key features, illustrated for the downstream domains in Figure 10. First, the spring low-flow statistic was generally similar to the baseline scenario (Figure 10A), though sometimes lower or higher due to removed influence of the reservoir-filling and -spilling. In the last panel (Figure 10A right), we see the difference between the high- and low-infiltration methods in Lower Valley. Variance is slightly wider for the high-infiltration method, consistent with the flashiness caused by a low water table. Note that unimpaired flow is the same as dam-removal shown here, except that it assumes infiltration is always low in Lower Valley, while dam-removal assumes it to be bracketed between low and high.

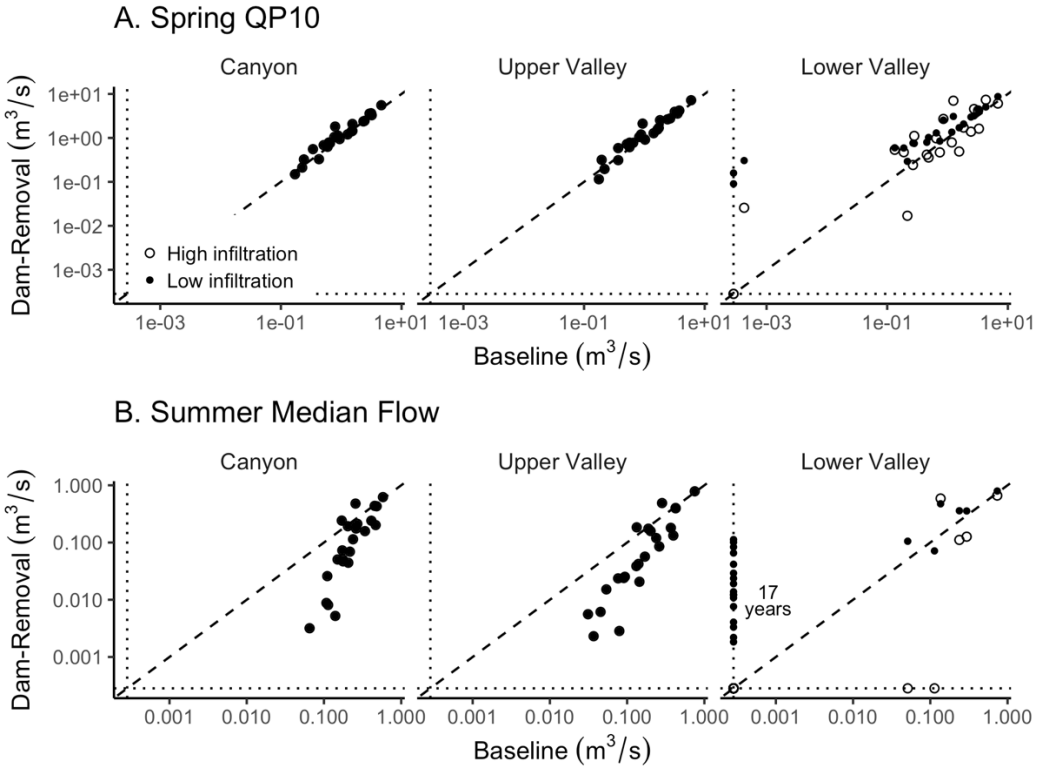

Figure 10. Dam-removal flow metrics, relative to the baseline. Large dots show where high- and low-infiltration methods are the same (Canyon & Upper Valley); small dots and circles show where they differ (Lower Valley). **A.** Spring QP_{10} is the predictor for length in the parr model. **B.** Summer median flow (QP_{50}) is the predictor for density in the parr model. Dotted axes show the minimum detectable flow at the gauge; symbols on these axes are estimates of zero flow.

The second key feature involved summer median flows in the Canyon and Upper Valley (Figure 10B, left and center). In wet years, baseline and dam-removal scenarios were similar, but in dry years the dam-removal scenario dropped to much lower levels. This implies that Los Padres Reservoir has maintained summer flows at unnaturally high levels, typical of many reservoirs in the arid southwest.

The third key feature is that this pattern reverses in the Lower Valley due to assumptions about groundwater. Seventeen years had zero flow in the baseline scenario, but maintained 0.002 to 0.03 m^3/s in the version of dam-removal with low-infiltration. This was comparable to Upper Valley. In the high-infiltration version, these seventeen years and another two went back to zero.

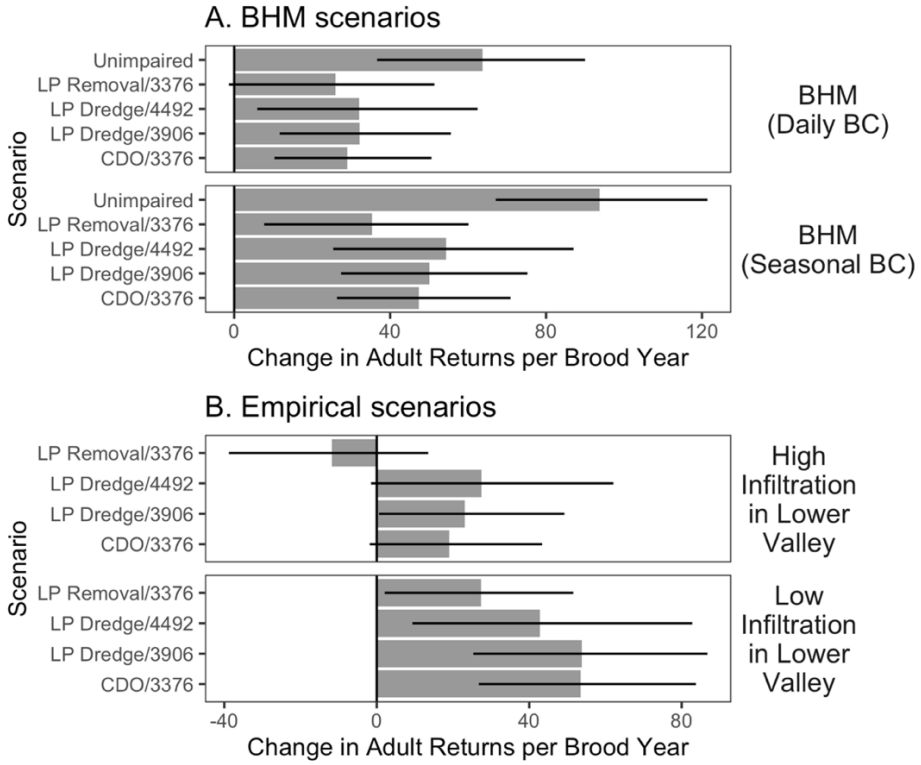

Figure 11. Predicted effects of water scenarios on adult steelhead returns, relative to baseline. Bars show median and 66% interval for responses of 23 brood years (1993-2015). **A.** Scenarios using the Basin Hydrologic Model (BHM), with two methods for bias-correction (BC; see Table 1). **B.** Empirical scenarios constructed using at-a-station regression models, and two bracketing assumptions for infiltration in the Lower Valley.

Steelhead population response

We report each scenario as the additional adults produced per brood year, relative to the baseline. For reference, the baseline had a median run of 388 spawners in this period. Note that all adult returns are calibrated as migrant counts at the former San Clemente Dam site; counts for the entire population are estimated to be about 75% higher (1/0.57 = 1.75; see Supplement §S2).

In the BHM scenarios (Figure 11A), the two bias-correction methods gave similar rankings among the scenarios, but the seasonal method generated bigger responses on an absolute scale. Unimpaired flows generated the strongest response, by a large margin; and dam-removal the weakest response, by a small margin. The CDO scenario performed slightly better than dam removal, and the two dam-expansion scenarios performed slightly better still. Overall these responses were on the order of 30-50 additional adult steelhead per year (50-90 for entire watershed), although the error bars indicate much year-to-year variability, and none performed as well as the unimpaired scenario.

The empirical scenarios (Figure 11B) rank similarly to the BHM scenarios, but their response is smaller overall, and indeed the response for dam-removal + high infiltration is negative—worse than the baseline scenario, which also has high infiltration but higher summer flows maintained by the reservoir. The establishment of low infiltration in Lower Valley produces a substantial positive response across all scenarios, such that the worst response (Dam Removal) is comparable to the best response under high infiltration (LP Dredge/4482). Note that the unimpaired scenario—omitted from Figure 11B—is identical to dam-removal/low infiltration.

Discussion

Our regression approach emphasized precision and out-of-sample prediction, but also realism within the constraints of generalized additive models. Findings were generally coherent and sensible, although not always expected.

Parr size and abundance both showed signs of a realistic, density-dependent response to spawner abundance, but flow also played a role, with minimum flows in spring predictive of parr size and median flows in summer predictive of parr density. Parr size and density themselves showed correlations consistent with self-thinning processes, suggesting that spring flow is the primary driver of parr growth, size, and—via self-thinning—density at the end of summer. This seems the most plausible explanation for the negative relationship between summer flow and parr density at the end of summer (Figure 6B), suggesting fish largely set up their spatial distribution by mid-summer.

The main role of summer flow appeared to be simply the maintenance of habitat area and connectivity. Longitudinal connectivity was largely maintained by keeping $QP_{10} > 0.10$ or 0.15 m^3/s, which also maintained a wetted width of 7 – 8 m on the mainstem. About one meter of wetted width was added for each additional 0.15 m^3/s (≈5 ft^3/s).

However, we cannot disprove a role for summer flow on fish growth, due to the limitations of the data and our approach: Spring flow was most predictive of size, but summer flow could also be predictive (we limited ourselves to one predictor), and of course spring and summer flow are correlated and therefore confounded in the dataset. Such confounding is always the case for uncontrolled experiments such as the water management scheme in Carmel River. In the Mediterranean climate of California, parr growth during the low-flow conditions of summer is often quite limited (Hayes et al. 2008; McCarthy et al. 2009; Kelson and Carlson 2019), but not everywhere (Rundio and Lindley 2008), and sometimes higher summer growth is associated with higher flow (Harvey et al. 2005). But typically, growth is fastest in winter and spring (Hayes et al. 2008; Sogard et al. 2009; Kelson and Carlson 2019), consistent with our finding.

Dam removal and dam rehabilitation

In the dam-removal and unimpaired scenarios, the summer low-flow metric routinely dropped below the threshold for connectivity (0.10 m^3/s) in both the Canyon and Upper Valley, whereas in the baseline it mostly stayed above it (Figure 10). These diminished summer flows partially explain the weak population response to dam-removal, although presumably the fish are adapted to these low flows since they also characterize the unimpaired scenario, and indeed are typical in coastal California (Hayes et al. 2008; Boughton et al. 2009).

Of course, dam-removal has other benefits for fish, including improved upstream passage for migrating adults, and especially the restoration of sediment regimes that reverse ongoing channel incision and more generally drive habitat-forming processes (Bednarek 2001; Tullos et al. 2014; East et al. 2015). For example, Harrison et al. (2018) found that after removal of San Clemente Dam from Carmel River, deposition of gravel enhanced steelhead spawning habitat downstream of the dam. Even so, a preponderance of sand as well as turbidity patterns during high-flow events suggested the river was still starved of gravel by Los Padres Dam (Harrison et al. 2018; Smith et al. 2021).

The dam-removal scenario also restored the 80% of parr that were assumed to disappear into the reservoir. Because these parr tended to be smaller than parr elsewhere, and only 17% of total accessible stream channel was above the dam, its removal generated surprisingly modest population responses. The various dam-rehabilitation scenarios generated slightly larger responses, mostly by maintaining continuous surface flow in the Lower Valley. Of these

rehabilitation scenarios, the biggest marginal gain was achieved simply by the water company obeying the law—relative to baseline, the scenario CDO/3376 added 20 to 50 adult steelhead per year across the various methods in Figure 11. Further expansion of the water right by reservoir dredging only adds an additional 10 adults at best, except when infiltration is low in the Lower Valley. Then it could add 25 to 45 more adults per year.

The Importance of Lower Valley

In fact, across all scenarios the population response was quite sensitive to infiltration conditions in Lower Valley (e.g. Figure 11B). This sensitivity rested on two specific factors: the Lower Valley had large parr—40% larger than the Canyon on average—and was vulnerable to loss of surface flow. Thus, scenarios that maintained perennial flow in the Lower Valley tended to generate outsized pulses of large parr that boosted adult returns, simply due to a larger wetted area.

Here is where the realism of the regression approach must be considered carefully. The occurrence of larger fish in the Lower Valley was also emphasized by Snider (1983) and Dettman and Kelley (1986), so it appears to be a consistent habitat association. Our statistical approach assumed that such fish would fill the available habitat (wetted area), which is also consistent with past observations. For example, before 1991 the entire Upper and Lower Valley dried out in most summers, but during the exceptionally wet year of 1982, when the river stayed relatively well connected to the estuary for the first time since at least 1960 (Figure 1a), Dettman and Kelley (1986) found large parr throughout the Lower Valley. So the two key factors driving the Lower Valley predictions are reasonable, although the underlying biological mechanism is unclear.

One potential mechanism is that faster-growing parr accumulate in the Lower Valley, either due to favorable growth conditions in this sort of alluvial channel (Moore 1980), or in the adjacent estuary (Bond 2006). Another potential mechanism is that age 1 fish tend to accumulate in the Lower Valley, due to downstream movements of age 0 parr the previous winter (Sogard et al. 2009; Kelson and Carlson 2019). The latter is consistent with extensive scale analyses reported by Dettman and Kelley (1986), who in the wet year 1982 found age 0 parr tended to predominate throughout the Carmel River system except in the Lower Valley, where age 1 parr predominated. In a small tributary of the South Fork Eel River with a similar mediterranean climate, Kelson and Carlson (2019) observed a distinct pulse of downstream parr movement during the first few rainstorms of the wet season, suggesting that this may be a common life-history strategy for *O. mykiss* in these sorts of seasonal rain-fed stream systems. Of course the two potential mechanisms of faster growth and age 1 habitat are not mutually exclusive

In our regression approach, we only modeled the predominant size class in each stream reach, and treated the influence of other size classes as random effects held constant across scenarios. This would tend to magnify the distinction between Lower Valley and the other domains, because in reality when Lower Valley is dry the age 1 fish might tend to accumulate throughout the other domains in a way that is not captured by our regression approach.

Yet continuous surface flow in Lower Valley appears to be an important predictor of large spawner abundances two and three years later. This pattern was reported by Arriaza et al. (2017), and the exceptionally wet year of 2017 reprised the pattern yet again, when sites in the Lower Valley had median parr size greater than 110 mm for the first time since 2000, and adult returns subsequently bumped up in 2019 and 2020 from earlier, very low levels. The very large effect of spring flow on fish size at end of summer (visible in Figure 6F for spring $QP_{10} > 3$ m^3/s) reflects

this pattern, because these wettest springs were the same years when the Lower Valley retained surface flow throughout the dry season.

Holding all else constant

By design our statistical approach was a conservative look at the effect of flow, holding all else constant including the rescued fish and the number of spawners. In reality wetter scenarios would tend to generate fewer strandings and require fewer fish rescues, but we held this effect constant. Interestingly, the number of rescued fish released into a domain was positively associated with density at end of summer ($p < 0.0001$), but not with size. This suggests that a substantial number of rescued fish survived to the end of summer, without imposing any negative effects on growth rates of *in situ* fish. This in turn implies asymmetric competition for food between the rescued and *in situ* fish, consistent with many conceptual models of salmonid ecology (e.g. Hughes 1998).

We also held spawner abundance constant, but in reality both the positive and negative effects of a scenario on spawner abundance would compound exponentially over multiple generations. Thus, our results are best viewed as a series of independent trials (one per year) than as a simulation of population dynamics. In a second set of simulations (not reported here), we included the compounding effect of spawner abundance but obtained a similar, though marginally more modest, response of the population to the various scenarios. Thus the positive and negative compounding effects of population growth and decline, respectively, appeared to roughly balance each other out.

Finally, our statistical approach focused on the most abundant age class at each sample reach, which for most sites is age 0 fish, but for sites in the Lower Valley is usually age 1 fish. The effect of age 1 fish elsewhere was treated as a random effect that was held constant, which may be simplistic.

Conclusions

To summarize, the population responses to the various dam-rehabilitation scenarios as well as to the dam-removal scenario were moderately positive and comparable in magnitude. Low-infiltration in the Lower Valley was at least as beneficial as the various dam scenarios for improving spawner abundance, and highlights the unique role of the Lower Valley in population productivity as well as the key importance of maintaining surface flow during the dry season. A substantial portion of variability in spawner abundance appears to be driven by spring flow conditions rather than summer flow conditions, via its effect on somatic growth in early life history.

Acknowledgements

We thank Cory Hamilton for sharing his extensive and always-informative insights about this fish population. Eric Danner reviewed the manuscript and provided helpful feedback. Staff of the Monterey Peninsula Water Management District generously responded quickly to numerous data requests, and California American Water provided financial support for data collection and analysis through a memorandum of understanding with the SW Fisheries Science Center. Finally, Amanda Ingham, Joel Casagrande, Thomas Wadsworth, Andres Ticlavilca, and David Crowder, all of the NMFS Coastal Office, were always available for insightful questions and discussion about the turning point facing the Carmel River steelhead population.

References

Adams, P. B., L. B. Boydstun, S. P. Gallagher, M. K. Lacy, T. McDonald, and K. E. Shaffer. 2011. California coastal salmonid population monitoring: strategy, design, and methods. Fish Bulletin. State of California, Department of Fish and Game 180:4-82.

Allendorf, F. W., D. Bayles, D. L. Bottom, K. P. Currens, C. A. Frissell, D. Hankin, J. A. Lichatowich, W. Nehlsen, P. C. Trotter, and T. H. Williams. 1997. Prioritizing Pacific salmon stocks for conservation. Conservation Biology 11(1):140-152.

Arriaza, J. L., D. A. Boughton, K. Urquhart, and M. Mangel. 2017. Size-conditional smolting and the response of Carmel River steelhead to two decades of conservation efforts. Plos One 12(11).

Ayllon, D., A. Almodovar, G. G. Nicola, I. Parra, and B. Elvira. 2012. Modelling carrying capacity dynamics for the conservation and management of territorial salmonids. Fisheries Research 134:95-103.

Bednarek, A. T. 2001. Undamming rivers: A review of the ecological impacts of dam removal. Environmental Management 27(6):803-814.

Bond, M. H. 2006. Importance of estuarine rearing to central California steelhead (*Oncorhynchus mykiss*) growth and marine survival. Master's thesis. University of California Santa Cruz, Santa Cruz, California.

Bond, M. H., S. A. Hayes, C. V. Hanson, and R. B. MacFarlane. 2008. Marine survival of steelhead (*Oncorhynchus mykiss*) enhanced by a seasonally closed estuary. Canadian Journal of Fisheries and Aquatic Sciences 65(10):2242-2252.

Boughton, D. A., P. Adams, E. Anderson, C. Fusaro, E. A. Keller, E. Kelley, L. Lentsch, J. Nielsen, K. Perry, H. M. Regan, J. J. Smith, C. Swift, L. Thompson, and F. Watson. 2007. Viability criteria for steelhead of the south-central and southern California coast. NOAA Technical Memorandum NMFS-SWFSC 407.

Boughton, D. A., D. Chargualaf, K. Liddy, T. Kahles, and H. A. Ohms. 2020. Carmel River steelhead fisheries report 2020. California American Water Company, Pacific Grove, CA.

Boughton, D. A., H. Fish, J. Pope, and G. Holt. 2009. Spatial patterning of habitat for *Oncorhynchus mykiss* in a system of intermittent and perennial streams. Ecology of Freshwater Fish 18:92-105.

Boughton, D. A., J. Nelson, and M. K. Lacy. 2022. Integration of steelhead viability monitoring, recovery plans and fisheries management in the southern coastal area. Fish Bulletin. State of California, Department of Fish and Game (182).

Burnham, K. P., and D. R. Anderson. 2002. Model selection and multimodel inference : a practical information-theoretic approach, 2nd ed. Springer-Verlag, New York.

Carle, F. L., and M. R. Strub. 1978. New method for estimating population-size from removal data. Biometrics 34(4):621-630.

Dettman, D. H., and D. W. Kelley. 1986. Assessment of the Carmel River steelhead resource. Volume I. Biological investigations. Prepared for the Monterey Peninsula Water Management District by D.W. Kelley & Associates, Newcastle, CA.

Dunham, J. B., and G. L. Vinyard. 1997. Relationships between body mass, population density, and the self-thinning rule in stream-living salmonids. Canadian Journal of Fisheries and Aquatic Sciences 54(5):1025-1030.

East, A. E., G. R. Pess, J. A. Bountry, C. S. Magirl, A. C. Ritchie, J. B. Logan, T. J. Randle, M. C. Mastin, J. T. Minear, J. J. Duda, M. C. Liermann, M. L. McHenry, T. J. Beechie, and P. B. Shafroth. 2015. Large-scale dam removal on the Elwha River, Washington, USA: River channel and floodplain geomorphic change. Geomorphology 228:765-786.

Einum, S., L. Sundt-Hansen, and K. H. Nislow. 2006. The partitioning of density-dependent dispersal, growth and survival throughout ontogeny in a highly fecund organism. Oikos 113(3):489-496.

Gelman, A., and J. Hill. 2007. Data analysis using regression and multilevel/hierarchical models. Cambridge University Press, Cambridge.

Grant, J. W. A., and D. L. Kramer. 1990. Territory size as a predictor of the upper limit to population-density of juvenile salmonids in streams. Canadian Journal of Fisheries and Aquatic Sciences 47(9):1724-1737.

Grant, J. W. A., S. O. Steingrimsson, E. R. Keeley, and R. A. Cunjak. 1998. Implications of territory size for the measurement and prediction of salmonid abundance in streams. Canadian Journal of Fisheries and Aquatic Sciences 55:181-190.

Harrison, L. R., A. E. East, D. P. Smith, J. B. Logan, R. M. Bond, C. L. Nicol, T. H. Williams, D. A. Boughton, K. Chow, and L. Luna. 2018. River response to large-dam removal in a mediterranean hydroclimatic setting: Carmel River, California, USA. Earth Surface Processes and Landforms DOI: 10.1002/esp.4464.

Harvey, B. C., J. L. White, and R. J. Nakamoto. 2005. Habitat-specific biomass, survival, and growth of rainbow trout (Oncorhynchus mykiss) during summer in a small coastal stream. Canadian Journal of Fisheries and Aquatic Sciences 62(3):650-658.

Hayes, S. A., M. H. Bond, C. V. Hanson, E. V. Freund, J. J. Smith, E. C. Anderson, A. J. Ammann, and R. B. Macfarlane. 2008. Steelhead growth in a small central California watershed: upstream and estuarine rearing patterns. Transactions of the American Fisheries Society 137(1):114-128.

Hughes, N. F. 1998. A model of habitat selection by drift-feeding stream salmonids at different scales. Ecology 79(1):281-294.

Kelson, S. J., and S. M. Carlson. 2019. Do precipitation extremes drive growth and migration timing of a Pacific salmonid fish in Mediterranean-climate streams? Ecosphere 10(3):e02618.

Lindley, S. T., R. S. Schick, E. Mora, P. B. Adams, J. J. Anderson, S. Greene, C. Hanson, B. P. May, D. R. McEwan, R. B. MacFarlane, C. Swanson, and J. G. Williams. 2007. Framework for assessing viability of threatended and endangered Chinook salmon and steelhead in the Sacramento-San Joaquin basin. San Francisco Estuary and Watershed Science 5(1):Article 4.

Matte, J.-M., D. J. Fraser, and J. W. A. Grant. 2020. Density-dependent growth and survival in salmonids: Quantifying biological mechanisms and methodological biases. Fish and Fisheries 21(3):588-600.

McCarthy, S. G., J. J. Duda, J. M. Emlen, G. R. Hodgson, and D. A. Beauchamp. 2009. Linking Habitat Quality with Trophic Performance of Steelhead along Forest Gradients in the South Fork Trinity River Watershed, California. Transactions of the American Fisheries Society 138(3):506-521.

McElreath, R. 2020. Statistical rethinking: A Bayesian course with examples from R and Stan. 2nd ed. Chapman and Hall/CRC, Boca Raton.

Montgomery, D. R. 1999. Process domains and the river continuum. Journal of the American Water Resources Association 35(2):397-410.

Montgomery, D. R., and J. M. Buffington. 1997. Channel-reach morphology in mountain drainage basins. Geological Society of America Bulletin 109(5):596-611.

Moore, M. R. 1980. Factors influencing the survival of juvenile steelhead rainbow trout (*Salmo gairdneri gairdneri*) in the Ventura River, California. Humboldt State University, Arcata, CA.

Myrvold, K. M., and B. P. Kennedy. 2015. Local habitat conditions explain the variation in the strength of self-thinning in a stream salmonid. Ecology and Evolution 5(16):3231-3242.

O'Donnell, D., A. Rushworth, A. W. Bowman, E. M. Scott, and M. Hallard. 2014. Flexible regression models over river networks. Journal of the Royal Statistical Society Series C-Applied Statistics 63(1):47-63.

Ogle, D. H., J. C. Doll, P. Wheeler, and A. Dinno. 2021a. FSA: Fisheries Stock Analysis.

Ogle, D. H., P. Wheeler, and A. Dinno. 2021b. FSA: Fisheries stock analysis. Version 0.8.32. https://github.com/droglenc/FSA.

Ohms, H. A., D. N. Chargualaf, G. Brooks, C. Hamilton, E. P. Palkovacs, and D. A. Boughton. 2022. Poor downstream passage at a dam creates an ecological trap for migratory fish. Canadian Journa of Fisheries and Aquatic Sciences Just In.

Pearse, D. E., N. J. Barson, T. Nome, G. T. Gao, M. A. Campbell, A. Abadia-Cardoso, E. C. Anderson, D. E. Rundio, T. H. Williams, K. A. Naish, T. Moen, S. X. Liu, M. Kent, M. Moser, D. R. Minkley, E. B. Rondeau, M. S. O. Brieuc, S. Rod Sandve, M. R. Miller, L. Cedillo, K. Baruch, A. G. Hernandez, G. Ben-Zvi, D. Shem-Tov, O. Barad, K. Kuzishchin, J. C. Garza, S. T. Lindley, B. Koop, G. H. Thorgaard, Y. Palti, and S. Lien. 2019. Sex-dependent dominance maintains migration supergene in rainbow trout. Nature Ecology & Evolution 3(12):1731-+.

R Development Core Team. 2021. R: A language and environment for statistical computing. R Foundation for Statistical Computing, Vienna, Austria.

Reynolds, J. B., and A. L. Kolz. 2013. Chapter 8, Electrofishing. A. V. Zale, D. L. Parrish, and T. M. Sutton, editors. Fisheries Techniques, Third Edition. American Fisheries Society, Bethesda, Marlyland.

Rosenfeld, J. S. 2014. Modelling the effects of habitat on self-thinning, energy equivalence, and optimal habitat structure for juvenile trout. Canadian Journal of Fisheries and Aquatic Sciences 71(9):1395-1406.

Rundio, D. E., and S. T. Lindley. 2008. Seasonal patterns of terrestrial and aquatic prey abundance and use by *Oncorhynchus mykiss* in a California coastal basin with a Mediterranean climate. Transactions of the American Fisheries Society 137(2):467-480.

Satterthwaite, W. H., M. P. Beakes, E. M. Collins, D. R. Swank, J. E. Merz, R. G. Titus, S. M. Sogard, and M. Mangel. 2009. Steelhead life history on California's central coast: insights from a state-dependent model. Transactions of the American Fisheries Society 138(3):532-548.

Smith, D. P., J. Schnieders, L. Marshall, K. Melchor, S. Wolfe, D. Campbell, A. French, J. Randolph, M. Whitaker, J. Klein, C. Steinmetz, and R. Kwan. 2021. Influence of a post-dam sediment pulse and post-fire debris flows on steelhead spawning gravel in the Carmel River, California. Frontiers in Earth Science 9:802825.

Snider, W. M. 1983. Reconnaissance of the steelhead resource of the Carmel River drainage, Monterey County. California Department of Fish and Game, Environmental Services Branch, Administrative Report No. 83-3, Sacramento, CA.

Sogard, S. M., T. H. Williams, and H. Fish. 2009. Seasonal patterns of abundance, growth, and site fidelity of juvenile steelhead in a small coastal California stream. Transactions of the American Fisheries Society 138(3):549-563.

Spence, B. C., E. P. Bjorkstedt, J. C. Garza, J. J. Smith, D. G. Hankin, D. Fuller, W. E. Jones, R. Macedo, T. H. Williams, and E. Mora. 2008. A framework for assessing the viability of threatened and endangered salmon and steelhead in the North-Central California Coast Recovery Domain. . NOAA Technical Memorandum NMFS-SWFSC 423.

Temple, G. M., and T. N. Pearsons. 2007. Electrofishing: backpack and drift boat. Pages 95-132 *in* D. H. Johnson, and coeditors, editors. Salmonid field protocols handbook: techniques for assessing status and trends in salmon and trout populations. American Fisheries Socieity, Bethesda, MD, USA.

Tredennick, A. T., G. Hooker, S. P. Ellner, and P. B. Adler. 2021. A practical guide to selecting models for exploration, inference, and prediction in ecology. Ecology 102(6):e03336.

Tullos, D. D., D. S. Finn, and C. Walter. 2014. Geomorphic and Ecological Disturbance and Recovery from Two Small Dams and Their Removal. Plos One 9(9).

Ward, B. R. 2000. Declivity in steelhead (Oncorhynchus mykiss) recruitment at the Keogh River over the past decade. Canadian Journal of Fisheries and Aquatic Sciences 57(2):298-306.

Ward, B. R., P. A. Slaney, A. R. Facchin, and R. W. Land. 1989. Size-biased survival in steelhead trout (*Oncorhynchus mykiss*) - Back-calculated lengths from adults scales compared to migrating smolts at the Keogh River, British Columbia. Canadian Journal of Fisheries and Aquatic Sciences 46(11):1853-1858.

Wood, S. N. 2003. Thin-plate regression splines. Journal of the Royal Statistical Society (B) 65(1):95-114.

Wood, S. N. 2004. Stable and efficient multiple smoothing parameter estimation for generalized additive models. Journal of the American Statistical Association 99(467):673-686.

Wood, S. N. 2017. Generalized Additive Models: An Introduction with R, 2 edition. Chapman and Hall/CRC.

Wood, S. N., N. Pya, and B. Säfken. 2016. Smoothing parameter and model selection for general smooth models (with discussion). Journal of the American Statistical Association 111:1548-1575.

Supplementary Material

S1. Spawner Counts

Spawners have been counted in Carmel River in three ways: annual counts at San Clemente Dam; annual counts at Los Padres Dam, and sporadic surveys of egg nests (redds).

The series of counts from the two dams omit downstream spawners, but we believe them each to be reliable indicators of relative abundance across years, for the following reasons: 1) The counts from the two dams are highly correlated (Figure S1); 2) the relative abundance of San Clemente vs Los Padres counts are about the same as the relative amount of habitat upstream of each dam, and 3) analysis of the redd surveys (see §S2 below) suggested that redd occurrence is similar across the Canyon domain (where San Clemente Dam was located) and the Upper Valley Domain (which is below the San Clemente site and thus represents fish not counted at the dam). Redd occurrence in Lower Valley appears to be systematically lower than in Upper Valley and Canyon (see §S2 below)

We used San Clemente counts to represent abundance, because they are more complete than Los Padres counts and more systematically collected than redd data. However, San Clemente Dam was removed in 2015, so we used the counts at Los Padres to infer counts at the San Clemente site from 2016 onward (see §S3 below). Based on redd surveys, we estimate that San Clemente counts represent about 57% of the total spawner abundance of the entire river system on average (see §S2 below).

S2. Analysis of Redd Surveys

Redd surveys were conducted sporadically by the local water district over the years, between Los Padres Dam and the estuary. Unfortunately, the haphazard sampling plan of these surveys makes them unsuitable for estimating true redd abundance, but we did assess how redd counts per reach vary among years, individual reaches, and process domains, including also the San Clemente adult counts as a covariate. The random effects of year and reach need to be interpreted cautiously because they reflect not just temporal and spatial variation in redd counts, but also the nuisance effects of the haphazard sampling plan. We assume the random effects capture these nuisance effects, and interpret fixed effects of process domain more confidently.

The redd data are zero-inflated, which means stream reaches observed to have zero redds occur disproportionately to other counts (nonzero), a common feature of population surveys. We thus analyzed the counts using a zero-inflated Poisson model (ZIP model; see mgcv::ziplss in the R package mgcv). The ZIP model has two linear predictors (regression equations). One predicts redd occurrence per sample reach using logistic regression (0 redds vs >0 redds), the other predicts redd abundance when they occur using Poisson regression (number of redds, given number of redds is > 0). Table S1 summarises the results.

Not surprisingly, spawner abundance was a significant predictor for both redd occurrence and redd abundance (Table S1C). Encouragingly, once this annual effect of spawner abundance was taken into account, the random effect of year on redd occurrence was not statistically significant ($p = 0.14$; Table S1B), suggesting that the haphazard sampling did not bias the annual mean occurrence. This was not the case for redd abundance ($p < 0.0001$), although this random effect of year could stem from a variety of sources, including flow conditions.

Focusing on the fixed effects of process domain (Table S1A), we see that average redd abundance in Lower Valley and in Upper Valley were not significantly different from average abundance in Canyon ($p = 0.57$ and $p = 0.56$, respectively).

Table S1. Terms of a generalized additive model for redd counts.

A. Fixed effects	**Estimate**	**SE**	***t***	***p***
Redd Abundance				
Intercept (Canyon)	0.5551	0.180	3.087	0.002
Lower Valley	-0.151	0.270	-0.562	0.57
Upper Valley	0.151	0.256	0.588	0.56
Redd Occurrence				
Intercept (Canyon)	-1.1055	0.1301	-8.4993	< 0.0001
Lower Valley	-0.6757	0.2033	-3.3233	0.0009
Upper Valley	0.1686	0.1952	0.8639	0.39
B. Random Effects	***edf***	**Ref. *df***	***F***	***p***
Redd Abundance				
Year	18.4	30.0	95.72	< 0.0001
Reach	71.9	140.0	352.3	< 0.0001
Redd Occurrence				
Year	4.3	30.0	5.62	0.14
Reach	83.0	165.0	164.7	< 0.0001
C. Smooth terms	***edf***	**Ref. *df***	***F***	***p***
Redd Abundance				
s(Spawners)	1.0	1.0	12.27	0.0005
Redd Occurrence				
s(Spawners)	4.7	5.3	70.93	< 0.0001

Redd occurrence, however, was similar between Canyon and Upper Valley ($p = 0.39$), but was significantly lower in Lower Valley ($p = 0.0009$). Recalling that the estimates for the occurrence portion of Table S1A are for logistic regression, after transformation the mean occurrence of redds per reach per survey is 0.265 for the Canyon + Upper Valley, but is only 0.144 for the Lower Valley. These values are difficult to interpret due to the haphazard sampling plan, but their relative rates are more meaningful because the different process domains probably suffer from similar sampling biases. The relative rate of redd occurrence is 0.545 (=0.144/0.265) in the Lower Valley, relative to the reaches upstream. This finding is consistent with the lower abundance of age 0 fish observed there (Figure 3), as well as the predominance of sandy channel in this domain prior to removal of San Clemente Dam. Sandy substrate is not suitable for steelhead spawning.

From this analysis, we can roughly estimate the bias of the San Clemente counts, which omit fish spawning downstream of the dam. If occurrence of redds is similar throughout the watershed, except in Lower Valley, then we predict the bias from the ratio of stream kilometers above and below the dam site, discounting kilometers in Lower Valley by 0.545. This calculation suggests that the fraction of total spawners counted at San Clemente averages about 0.57.

S3. San Clemente Counts after 2015

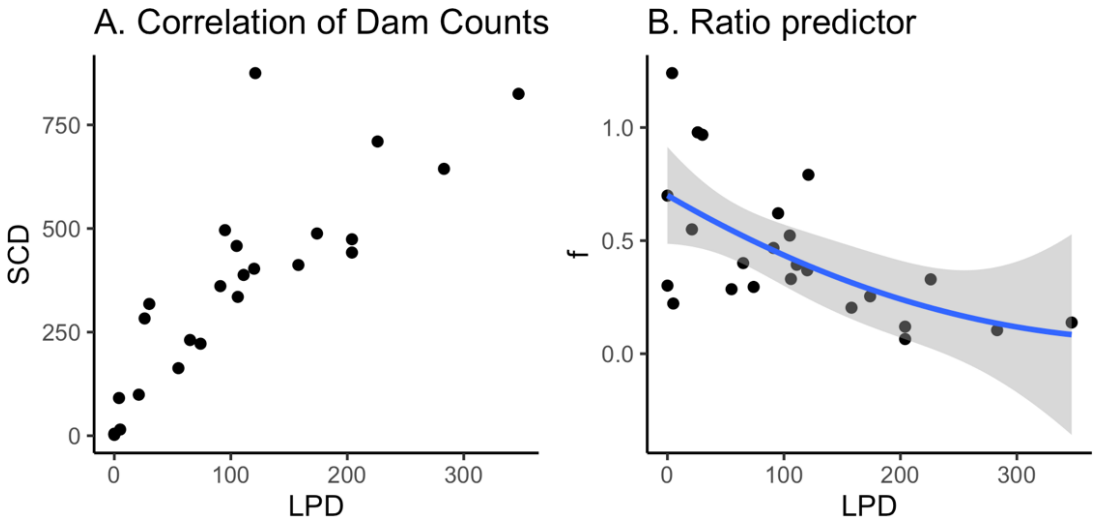

Figure S1. **A.** Counts of adult steelhead at San Clemente Dam (SCD) and Los Padres Dam (LPD), prior to removal of San Clemente Dam in 2015. Zero counts at both sites prior to 1992 are omitted. **B.** The ratio predictor *f* with the fitted second-order prediction line, used to infer SCD counts after 2015.

We used the counts of adult steelhead at the San Clemente Dam fish-ladder as the primary indicator for population response, in accordance with general NMFS practice of using adult abundance as an indicator for population risk status (Allendorf et al. 1997; Boughton et al. 2007; Lindley et al. 2007; Spence et al. 2008). These counts are biased low in that they omit adults who spawned downstream of San Clemente Dam, but are still the most reliable indicator for adult abundance of the population. However, San Clemente Dam was removed in 2015 so we need to somehow infer counts for 2016 onward. Fortunately, the counts at San Clemente are highly correlated with the counts at Los Padres (Figure S1A), so we can use the latter to predict the former.

In principle we could simply fit a regression to the points in Figure S1A, but we found the properties for the residual variance were better if modeled the predictor as a ratio,

Eq. S1 $$f = log_{10}\left(\frac{SCD-LPD}{LPD+1}\right),$$

which is plotted in Figure S1B. This equation simply represents the ratio of fish spawning above Los Padres Dam versus between the two dams, modified by adding 1 to the denominator and log-transforming, so as to stabilize the variance near zero. Since most of our counts after 2015 are small numbers, we want it to perform well near zero. Once we have fit a regression to *f*, we use it to predict spawner abundance from the counts at Los Padres Dam, using the reverse equation:

Eq. S2 $$N = round([LPD + 1]10^{f} + LPD)$$

Other advantages of this approach are that the predicted counts at San Clemente are always greater or equal to the counts at Los Padres, and the predictor accounts for the fact that prediction

error only occurs for the fish spawning between the two dams, not for the fish spawning above Los Padres.

Curvature in the point cloud can be observed in both panels of Figure S1, so we fit a second-order polynomial regression to predict *f*, illustrated in Figure S1B. The predicted values of *f* and *N* for 2016 onward are in Table S2.

Table S2. Predictors and predictions for spawner abundance after the removal of San Clemente Dam.

Year	**LPD**	***f***	***N***
2016	0	0.70	5
2017	7	0.68	45
2018	29	0.62	153
2019	126	0.38	430
2020	65	0.52	284

S4. Addressing "the Zero Problem" for Bias-Correction of Daily Flows

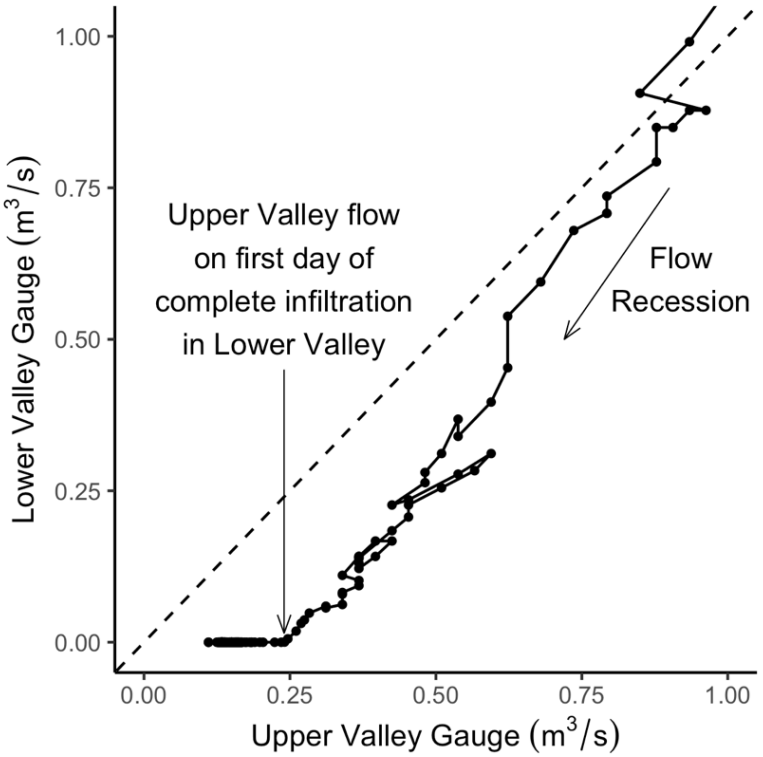

Figure S2. An example of "the zero problem" from summer 1997, where each dot is same-day daily flow at the two gauges, and the lines connect them as a time series. As daily flow recedes over the course of the summer, the disparity (distance from dashed line) widens between the Upper Valley gauge (*x*-axis) and Lower Valley gauge (*y*-axis), due to infiltration. The vertical arrow marks a transition point below which all surface flow at Upper Valley infiltrates before Lower Valley. Below this transition, the key assumption of the bias-correction method is not valid.

In addition to the bias-correction method of Eq. 5, we also addressed the "zero problem" in Lower Valley caused by its low water table and high infiltration rate (Figure S2). The modeled baseline never predicted zero flow, a clear mismatch from reality in Lower Valley that implies infiltration and water-table dynamics were not well represented by the BHM. Our bias-correction method cannot address this, but a simple statistical fix is to assume that the Lower Valley has a fixed daily infiltration capacity, and to estimate it as the highest flow at Upper Valley that had zero flow observed at Lower Valley (vertical arrow in Figure S2). To use this assumption in the seasonal bias correction, we replaced the zeros at Lower Valley with the corresponding metric at Upper Valley, subtacted the infiltration capacity, and then applied Eq. 5. If the resulting value was positive, we assumed net surface flow that overcame the infiltration capacity of Lower Valley; if it was negative we assumed it all went into the aquifer and set the metric to zero. For the daily version of bias correction, we did the same but assumed a distinct infiltration capacity each year, estimated as the flow at Upper Valley on the first day each year where flow was zero at Lower Valley.

This statistical approach may be somewhat optimistic, since it assumes that infiltration capacity is fixed over the dry season, when in fact the water table is probably being progressively drawn down by continued water withdrawals.

Table S3. Estimated terms of the spawner model

Predictor[1]	**Coefficient**	**SE**	***t***	***p***
Parr Abundance (N)	0.00181	0.00014	13.4	$<10^{-11}$
Fork Length (mm)	0.83	9.04	0.092	0.93
Interaction	0.000096	0.000043	2.23	0.036

[1] Fork length predictor centered on the grand mean of all reaches in all years (80.9 mm), so parr coefficient represents survival of a cohort whose mean fork length is 80.9 mm.

S5. Partial effects and reconstructed hydrographs from at-a-station models

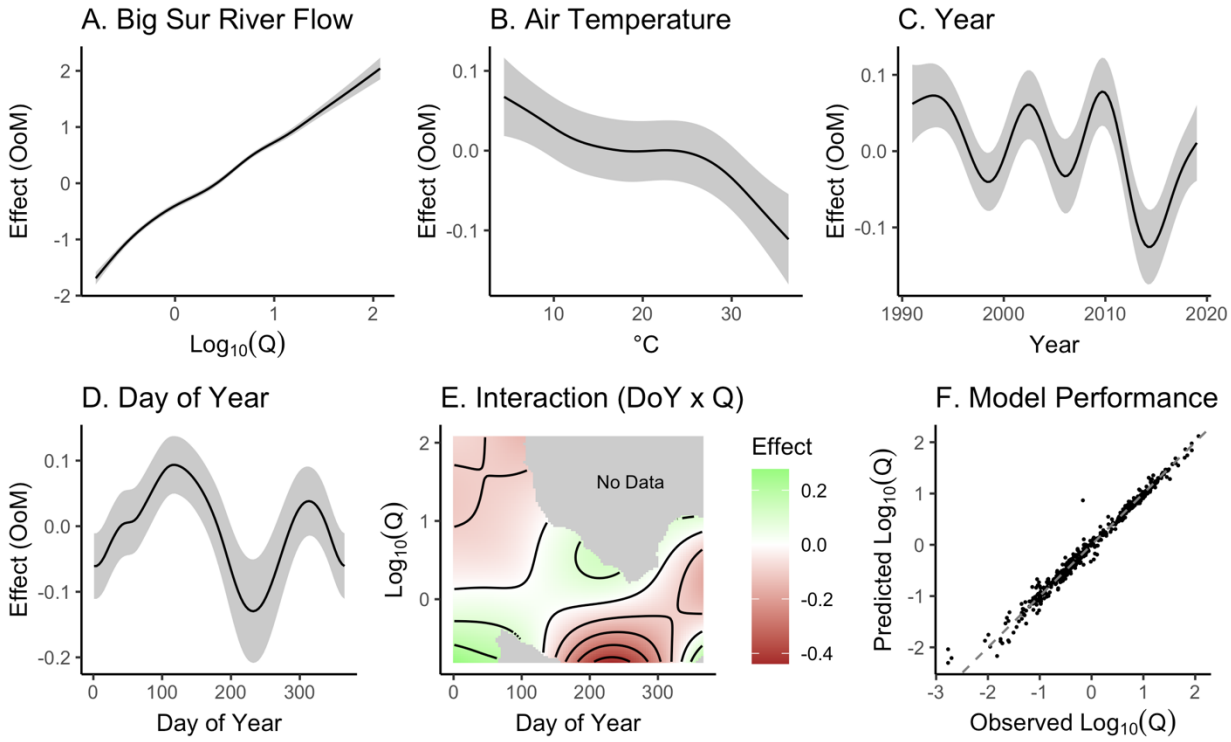

Figure S3. Partial effects for unimpaired flow above Los Padres Reservoir (LP gauge). The main predictor for flow was daily gauge data from the Big Sur River (**A**), but air temperature (**B**), implicit annual trends (**C**) and implicit seasonal trends (**D**) were also selected as predictors. Vertical axis "OoM" is Order of Magnitude.

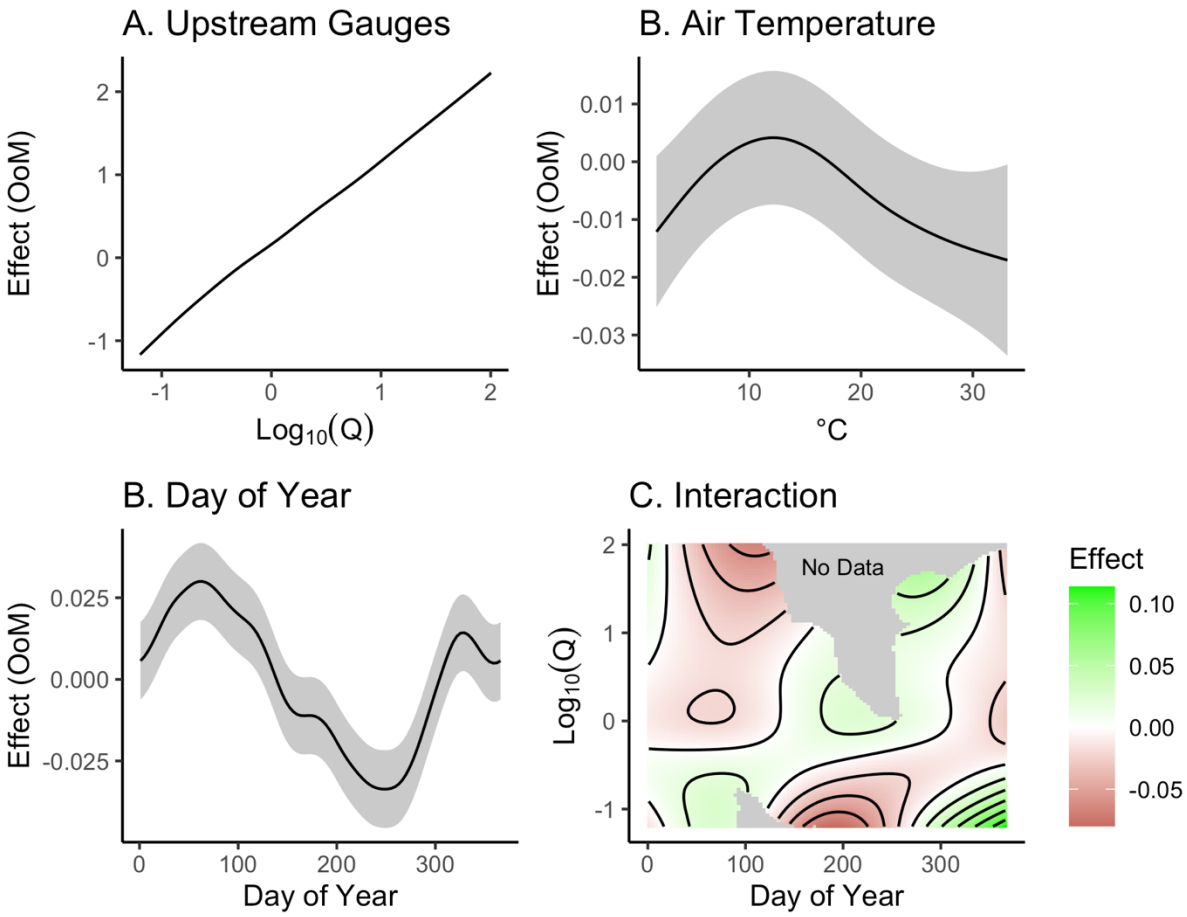

Figure S4. Regression terms for predicting flow in the Canyon (SH gauge) from upstream gauges (**A**). Mean air temperature (**B**), implicit seasonal trends (**C**) and one two-interaction (**D**) were also selected as predictors. Vertical axis "OoM" is Order of Magnitude. The main upstream gauge (BL, releases from Los Padres Reservoir) has no data prior to 2001, so a smooth year term was omitted from the model.

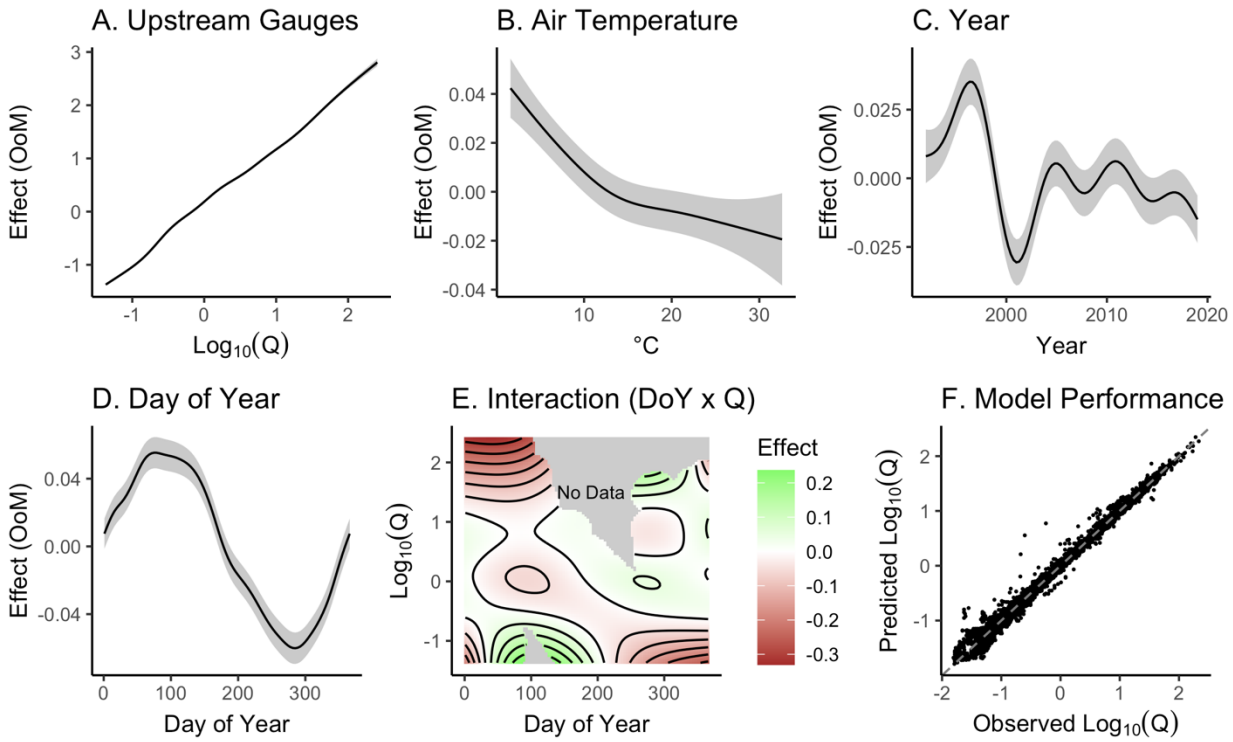

Figure S5. Regression terms for predicting flow in the Upper Valley (DJ gauge) from upstream gauges (**A**). Mean air temperature (**B**), implicit annual trends (**C**), implicit seasonal trends (**D**), and one two-interaction (**E**) were also selected as predictors. Vertical axis "OoM" is Order of Magnitude.

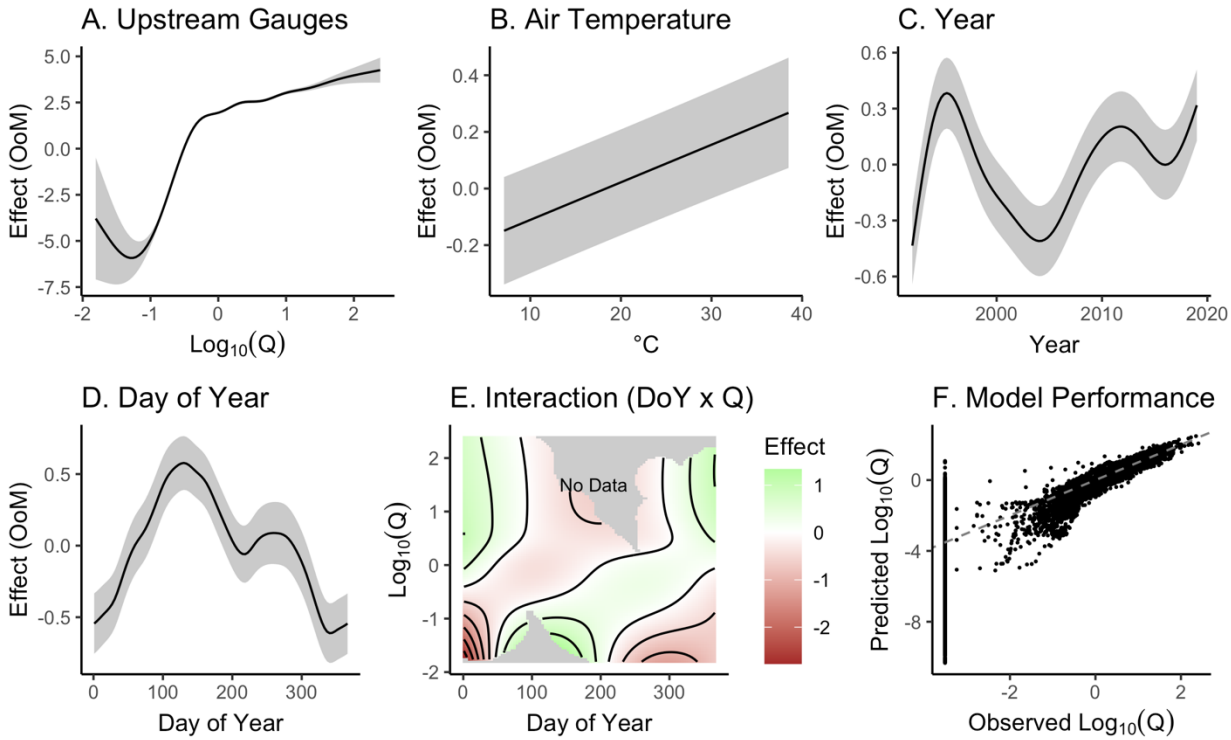

Figure S6. Regression terms for predicting flow in the Lower Valley (NC gauge) from upstream gauges (**A**). Mean air temperature (**B**), implicit annual trends (**C**), implicit seasonal trends (**D**), and a two-interaction (**E**) were also selected as predictors. Vertical axis "OoM" is Order of Magnitude. The link function of the regression model was a censored tobit distribution to handle the numerous zero observations in the Lower Valley.

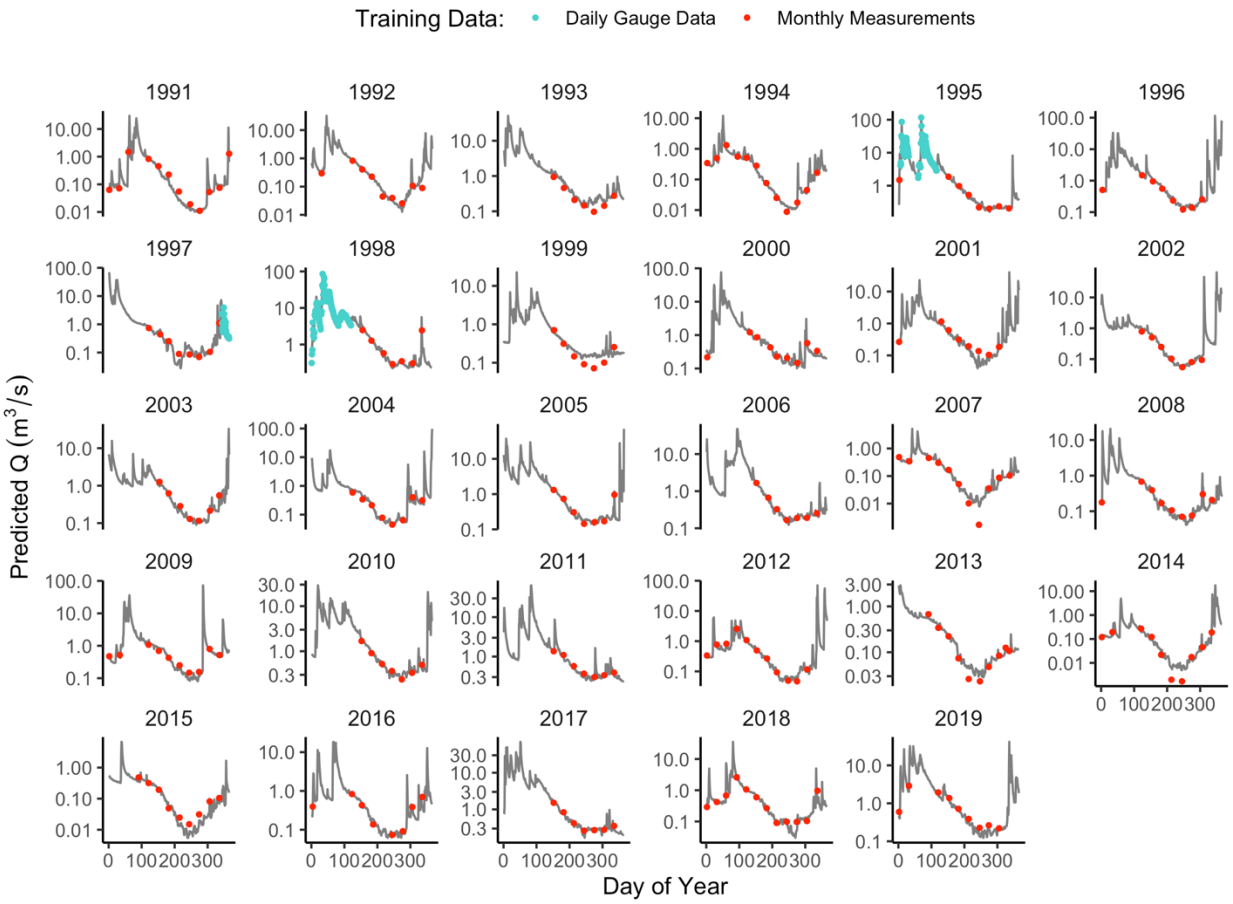

Figure S7. Reconstructed unimpaired flow at Los Padres Reservoir (gray), based on training data (circles) from measurements upstream of the reservoir.

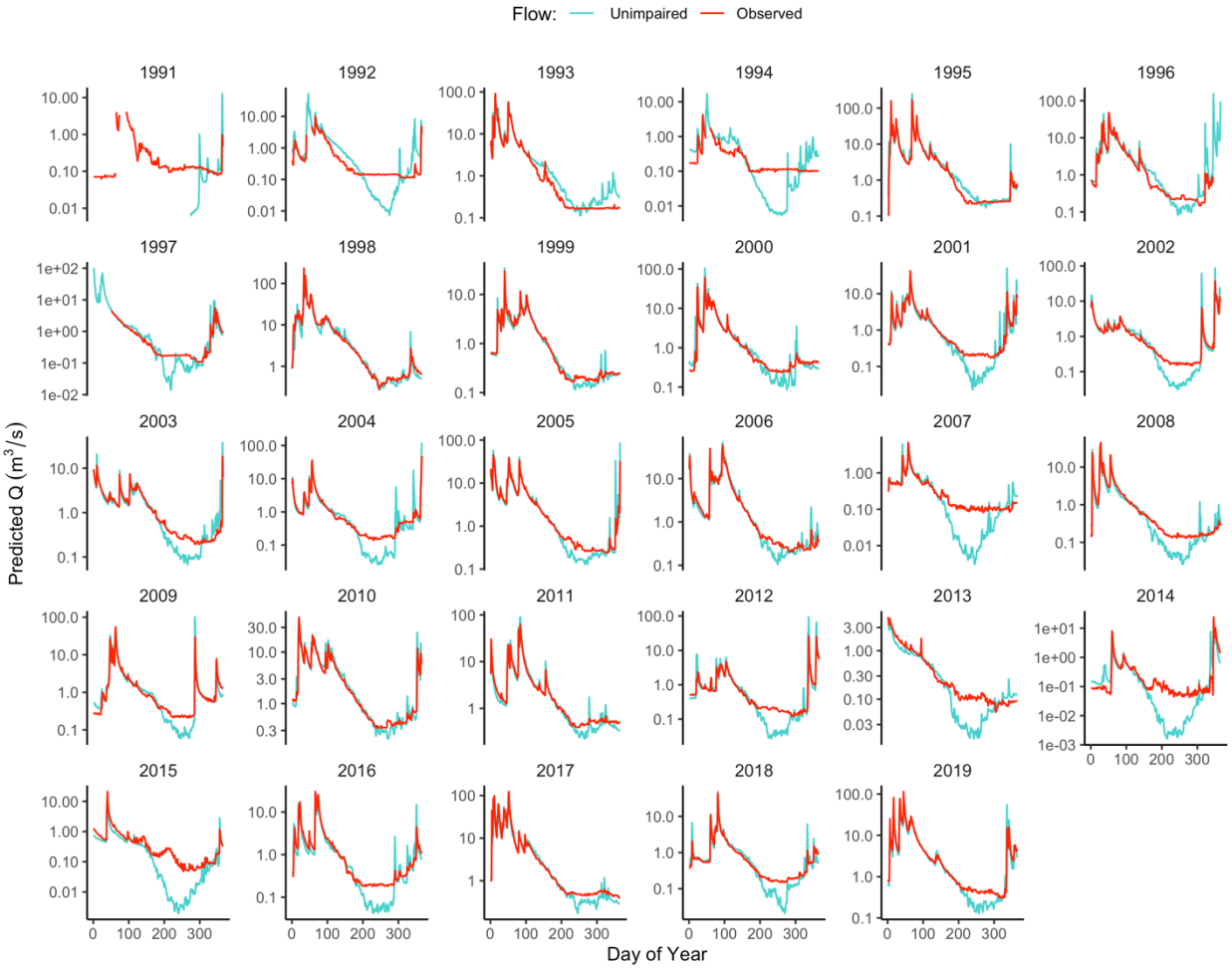

Figure S8. Empirical hydrographs in the Canyon Domain (Sleepy Hollow gauge), for the baseline scenario (red) and the unimpaired/dam-removal scenario (blue).

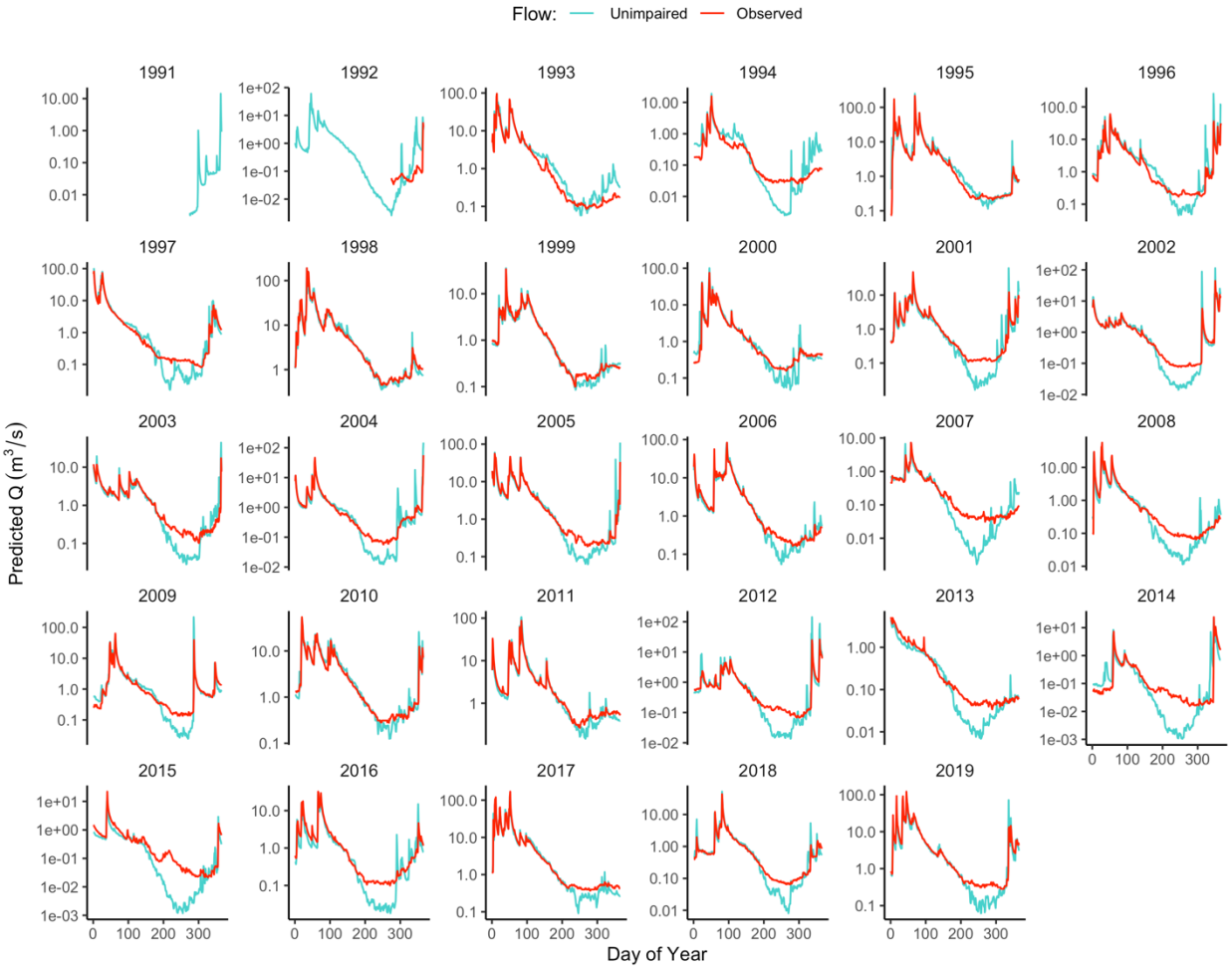

Figure S9. Empirical hydrographs in the Upper Valley Domain (Don Juan gauge), for the baseline scenario (red) and the unimpaired/dam-removal scenario (blue).

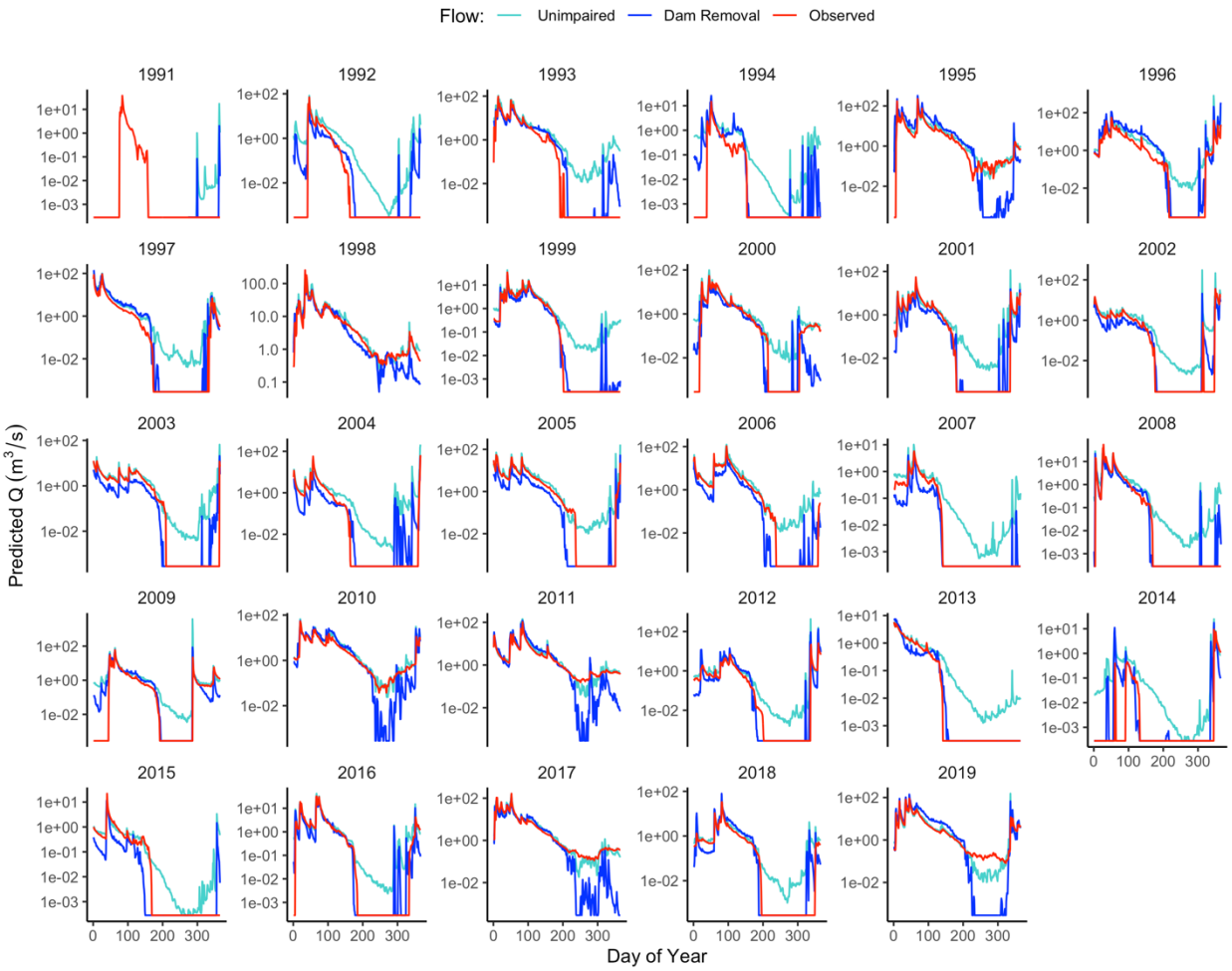

Figure S10. Empirical hydrographs in the Lower Valley Domain (Near Carmel gauge), for the baseline scenario (red), the unimpaired scenario (light blue), and the dam-removal scenario (dark blue).